

MATHEMATISCHES FORSCHUNGSINSTITUT OBERWOLFACH

Report No. 29/2022

DOI: 10.4171/OWR/2022/29

Hilbert Complexes: Analysis, Applications, and Discretizations

Organized by

Ana M. Alonso Rodriguez, Trento

Douglas N. Arnold, Minneapolis

Dirk Pauly, Dresden

Francesca Rapetti, Nice

19 June – 25 June 2022

ABSTRACT. In this workshop 70 (43 at MFO, 27 online) leading mathematicians from Europe, United States, China, and Australia met at the MFO to discuss and present new developments in the mathematical and numerical analysis including discretizations of Hilbert complexes related to systems of partial differential equations, in particular the well known de Rham complex and the complexes of elasticity and the biharmonic equations. The report at hand offers the extended abstracts of their talks.

Mathematics Subject Classification (2020): 35Axx, 35Jxx, 35Qxx, 47Bxx, 58Axx, 58Jxx.

Introduction by the Organizers

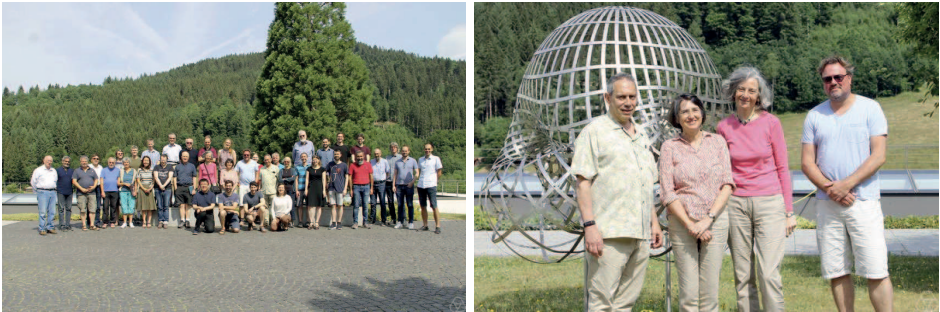
The workshop *Hilbert Complexes: Analysis, Applications, and Discretizations*, organised by Ana Alonso (Trento), Doug Arnold (Minneapolis), Dirk Pauly (Dresden), and Francesca Rapetti (Nice) was well attended with over 40 participants and over 25 additional online participants with broad geographic representation from Europe and the United States. This workshop was a nice blend of researchers with various backgrounds in mathematical and numerical analysis, applications, and discretizations of Hilbert Complexes, mainly in PDE related complexes.

Hilbert complexes arise throughout mathematical physics. The fundamental partial differential operators from which most models in continuum physics are built may be realized as unbounded operators mapping between Sobolev and related Hilbert spaces, and these spaces and operators assemble into chain complexes. The resulting structure is a Hilbert complex: a finite sequence of Hilbert spaces

together with closed unbounded operators from one space to the next such that the composition of two consecutive operators vanishes. This is a rich structure which combines functional analysis and homological algebra. Hilbert complexes arise not only in physics – electromagnetics, fluid mechanics, elasticity, general relativity, etc. – but are also fundamental to parts of geometry, such as the Hodge theory of Riemannian manifolds. In recent decades it has been discovered that the Hilbert space structure is crucial to numerical analysis as well. Stable discretization of the partial differential equations related to Hilbert complexes depends crucially on retaining the Hilbert space structure at the discrete level. This viewpoint has led to major advances in discretization for numerous problems, and holds great promise for other applications.

The de Rham complex – whether presented on a domain in space in terms of vector calculus, or more generally, in terms of differential forms on Riemannian manifolds – is a canonical example of a Hilbert complex, and many aspects of its analysis, application, and discretization are well-understood. The situation is less developed for other Hilbert complexes which arise in applications such as elasticity, plate theory, and general relativity. In particular, a systematic approach to deriving discretizations for these applications is not yet at hand. In view of the many applications, this would be of immense utility.

Interest in Hilbert complexes blurs the lines between analysis, geometry, numerical analysis, and applications, between pure and applied mathematics. In this workshop, we brought together researchers with an interest in Hilbert complexes and their implications coming from all these communities in order to establish new lines of communications and advance the state of the art.



Acknowledgement: The MFO and the workshop organizers would like to thank the National Science Foundation for supporting the participation of junior researchers in the workshop by the grant DMS-1641185, “US Junior Oberwolfach Fellows”.

Workshop: Hilbert Complexes: Analysis, Applications, and Discretizations

Table of Contents

Douglas N. Arnold	
<i>What are complexes doing in numerical PDE?</i>	1607
Kaibo Hu	
<i>Discretization of Hilbert complexes</i>	1610
Snorre H. Christiansen	
<i>Finite element systems</i>	1616
Evan S. Gawlik (joint with Yakov Berchenko-Kogan)	
<i>Finite elements for Riemannian geometry</i>	1617
Michael Neilan (joint with Johnny Guzmán, Anna Lischke)	
<i>Smooth finite element sequences on Worsey-Farin splits</i>	1620
Ralf Hiptmair (joint with Dirk Pauly and Erick Schulz)	
<i>Traces for Hilbert Complexes</i>	1622
Erick Schulz (joint with Ralf Hiptmair and Stefan Kurz)	
<i>Boundary Integral Exterior Calculus</i>	1625
Ari Stern (joint with Gerard Awanou, Maurice Fabien, and Johnny Guzmán)	
<i>Hybridization and postprocessing in finite element exterior calculus</i>	1628
Ragnar Winther (joint with Richard S. Falk)	
<i>The bubble transform and the de Rham complex</i>	1629
Francesca Bonizzoni (joint with Kaibo Hu, Guido Kanschat, Duygu Sap)	
<i>BGG sequences of tensor product finite elements with arbitrary continuity</i>	1631
Joachim Schöberl	
<i>Matrix-valued Finite Elements with Applications in</i> <i>Elasticity and Curvature</i>	1633
Michael Neunteufel (joint with Jay Gopalakrishnan, Joachim Schöberl, Max Wardetzky)	
<i>Analysis of curvature approximations via covariant curl and</i> <i>incompatibility for Regge metrics</i>	1637
Yakov Berchenko-Kogan	
<i>Duality and symmetry in finite element exterior calculus</i>	1639
Jay Gopalakrishnan (joint with Snorre Christiansen, Johnny Guzmán, Kaibo Hu)	
<i>Discrete Elasticity Complex on Alfeld Splits</i>	1640

Leszek Demkowicz, Stefan Henneking	
<i>The hp3D Code with Applications to Modeling of Optical Amplifiers</i> . . .	1643
Anil N. Hirani (joint with Daniel Berwick-Evans, Mark Schubel)	
<i>Discrete Vector Bundles with Connection and Curvature</i>	1646
Oliver Sander (joint with Hanne Hardering, Lisa Julia Nebel, and Patrizio Neff)	
<i>Geometric finite elements for nonlinear Cosserat shell problems</i>	1648
Sanna Mönkölä (joint with Lauri Kettunen, Tuomo Rossi, Jukka Rabinä, Tytti Saksa, and Jonni Lohi)	
<i>Numerical Simulation of Wave Equations</i>	1649
Lauri Kettunen, Tuomo Rossi	
<i>Towards “all” boundary value problems – exploitation of the structural properties</i>	1652

Abstracts

What are complexes doing in numerical PDE?

DOUGLAS N. ARNOLD

As an introduction to the workshop “Hilbert Complexes: Analysis, Applications, and Discretizations,” held in June 2022 at Oberwolfach, this talk began with the question: How did Hilbert complexes, mathematical objects which at first consideration may seem to be very distant from numerical analysis, come to play a major role in numerical PDE?

Topological background material. We began with a very quick review of the basic notions of topology and differential geometry needed. One simple but essential notion is that of a chain complex—a sequence of vector spaces V_k connected by linear maps $\partial_k : V_k \rightarrow V_{k-1}$ which are *differentials* in the sense that $\partial_{k-1} \circ \partial_k = 0$:

$$\cdots \rightarrow V_{k+1} \xrightarrow{\partial_{k+1}} V_k \xrightarrow{\partial_k} V_{k-1} \rightarrow \cdots$$

Similarly we introduced *cochain complexes*, *subcomplexes*, *chain maps*, and, most importantly, the notions of cycles and boundaries (kernels and ranges of the differential), and their quotient space, boundaries modulo cycles, which define the *homology spaces* of the chain complex.

A concrete example which explains some of the terminology is the *simplicial chain complex* which can be defined whenever we are given a simplicial complex, i.e., a triangulation (by simplices) of a domain in \mathbb{R}^n or a manifold. The spaces V_k consist of the k -dimensional chains in the simplicial complex, and ∂_k to be the boundary operator taking a k -chain to a $(k-1)$ -chain. The dimensions of the homology groups give the Betti numbers, which count the k -dimensional holes in the domain and are the most fundamental topological invariants.

The de Rham complex. A second example of a chain complex is the de Rham cochain complex for a domain $\Omega \subset \mathbb{R}^n$ (or a manifold). Here the spaces are $V^k = \Lambda^k(\Omega) := C^\infty(\Omega, \text{Alt}^k \mathbb{R}^n)$, the space of smooth *differential k -forms* on Ω and the differential $d^k : \Lambda^k(\Omega) \rightarrow \Lambda^{k+1}(\Omega)$ is the *exterior derivative*, the extension to any manifold of any dimension of the fundamental vector calculus operators grad, div, and curl. Now the de Rham complex is a cochain complex whose spaces are infinite dimensional function spaces and whose differentials are differential operators, so quite different from the simplicial chain complex, with finite dimensional spaces and combinatorial differentials. But their homology is the same. This is the content of De Rham’s Theorem. In particular, the de Rham cohomology spaces have the Betti numbers as their dimensions, just as for the simplicial chain complex.

The de Rham complex

$$(1) \quad 0 \rightarrow C^\infty \Lambda^0 \xrightarrow{d} C^\infty \Lambda^1 \xrightarrow{d} \cdots \xrightarrow{d} C^\infty \Lambda^n \rightarrow 0$$

is a simple, elegant homological structure which can be defined on any smooth manifold and which captures basic topological properties of the manifold. Its

differentials are exterior derivatives, which are fundamental first order partial differential operators from vector calculus. But it does not lead to other partial differential operators, since the only way to combine two exterior derivatives is by composition of two successive ones, which simply gives zero.

Hodge theory. To introduce *Hodge theory* we require additional structure of the domain or manifold, namely it must be a *Riemannian manifold*, i.e., at each point of the manifold, the tangent space is endowed with an inner product, depending smoothly on the point. Then we can define the L^2 spaces of differential forms, $L^2\Lambda^k$, which we take for the spaces in a complex. The operators are taken to be, again, the exterior derivatives, but these are now viewed as *closed, densely-defined linear operators* from $L^2\Lambda^k$ to $L^2\Lambda^{k+1}$ and so, instead of the smooth de Rham complex (1), we get the L^2 de Rham complex

$$(2) \quad 0 \rightarrow L^2\Lambda^0 \xrightarrow{d} L^2\Lambda^1 \xrightarrow{d} \dots \xrightarrow{d} L^2\Lambda^n \rightarrow 0.$$

We emphasize that the operator d^k here is only defined on a dense subspace of $L^2\Lambda^k$ and is not bounded. The property of being closed is a generalization of boundedness to operators which are only densely-defined.

Hilbert complexes. Just as the simplicial chain complex of a triangulation inspired the definition and study of the abstract structure named a chain complex, in which the spaces no longer need to refer to any triangulation, so the L^2 de Rham complex (2) inspired the abstract notion of a Hilbert complex, which is simply defined to be a sequence of Hilbert spaces W^k , with closed densely-defined linear operators $W^k \rightarrow W^{k+1}$ such that range of d^k is contained in the null-space of d^{k+1} . This definition was first promulgated by Brüning and Lesch in 1992 and first introduced into numerical analysis by Arnold, Falk, and Winther in 2010. Despite the simplicity of the definition, many of the key results of the Hodge theory of Riemannian manifolds can be proven within the framework of Hilbert complexes. An important example is the existence of a dual complex with the same spaces W^k , but with the maps $d_{k+1}^* : W^{k+1} \rightarrow W^k$ equal to the Hilbert space adjoint of $d^k : W^k \rightarrow W^{k+1}$ and so going in the opposite direction. Unlike the d^k alone, the d^k together with the d_k^* can be combined to create many important differential operators. The most canonical of these is the Hodge Laplacian $\Delta = dd^* + d^*d$, that is, $\Delta^k = d^{k-1}d_k^* + d_{k+1}^*d^k : L^2\Lambda^k \rightarrow L^2\Lambda^k$. The Hodge Laplacian operator was originally defined on differential k -forms on a manifold, but the definition and many of its properties extend to any closed Hilbert complex (here closed means that the range of each d^k is closed in W^{k+1}). Other properties of the de Rham complex on a Riemannian manifold which are best understood in the Hilbert complex framework are: the identification of the k th cohomology space with the space of harmonic k -forms, defined as the elements of W^k belonging to the null space of the Hodge Laplacian; the Hodge decomposition of the space W^k into three orthogonal subspaces, the range of d^{k-1} , the range of d_{k+1}^* , and the harmonic k -forms; and the Poincaré inequality.

Other examples of important Hilbert complexes. The elasticity complex (or Calabi complex or Kröner complex) is

$$0 \rightarrow L^2 \otimes \mathbb{V} \xrightarrow{\text{def}} L^2 \otimes \mathbb{S} \xrightarrow{\text{inc}} L^2 \otimes \mathbb{S} \xrightarrow{\text{div}} L^2 \otimes \mathbb{V} \rightarrow 0, \quad [\mathbb{V} := \mathbb{R}^3, \mathbb{S} := \mathbb{R}_{\text{symm}}^{3 \times 3}]$$

Here $\mathbb{V} = \mathbb{R}^3$, $\mathbb{S} = \mathbb{R}_{\text{symm}}^{3 \times 3}$. PDEs coming from this complex include the equations of elasticity in either primal or mixed form, and equations relating to general relativity. Note that the Saint Venant incompatibility operator $\text{inc} = \text{curl} T \text{curl}$ is *second order*.

The *Hessian complex* also contains a second order operator:

$$0 \rightarrow L^2 \xrightarrow{\text{hess}} L^2 \otimes \mathbb{S} \xrightarrow{\text{curl}} L^2 \mathbb{T} \xrightarrow{\text{div}} L^2 \otimes \mathbb{V} \rightarrow 0$$

with \mathbb{T} denoting the trace-free subspace of $\mathbb{R}^{3 \times 3}$. It relates to numerous PDEs, such as the biharmonic equation. Similarly we have the *div div complex*, which is adjoint to the Hessian complex, and has other applications.

The BGG construction. To apply these Hilbert complexes, we must establish some basic properties. The key one, that implies many other is that they are *closed* Hilbert spaces (the differentials have closed range). For the de Rham complex on a Lipschitz manifold with or without boundary, the closed ranges were established by R. Picard in 1984. Following Arnold and Hu 2021, in the talk we summarize a construction that allows us a systematic derivation of new complexes, starting with already known complexes. We call the construction the *BGG construction*, recognizing that it is related to the Bernstein–Gelfand–Gelfand resolution from representation theory of Lie algebras. Beginning with the de Rham complex, for example, we may derive, the Hessian complex, the *div div complex*, and many others. Moreover we can establish basic properties of these complexes based on known properties of the de Rham complex.

Discretization. Finally, we discuss the discretization of Hilbert complexes and PDEs arising from them. For any $k > 0$, the k -form Hodge Laplacian of any Hilbert complex is a naturally a saddle point formulation, and discretizing it stably requires developing special purpose finite elements suited to the type of space being discretized. For example, the 3-form Hodge Laplacian in 3 dimensions is the mixed variational formulation of the scalar Laplacian, written in terms of the flux. The flux belongs to the domain of d^2 in $L^2 \Lambda^2$, which is essentially the space $H(\text{div})$. The canonical finite elements to discretize $H(\text{div})$ are the Raviart–Thomas–Nédélec element—they are the canonical flux element. In fact, canonical stable finite element spaces have been designed *systematically* for all the fields arising from de Rham complex, i.e., for all of the differential form spaces in any number of dimensions. Indeed, these are captured in the Periodic Table of the Finite Elements (Arnold–Logg 2014), which is itself a major outcome of Finite Element Exterior Calculus.

In the final portion of the talk we show how the BGG construction can be used to discretize fields of different sorts, deriving new finite elements from old ones, and pointing the way to many new elements, a number of which have already been discovered.

Discretization of Hilbert complexes

KAIBO HU

Discretization of Hilbert complexes plays a central role in finite element exterior calculus [3, 6, 7]. In this report, we review some recent development in this direction, emphasizing conforming finite elements.

Overview. The overall aim of discretizing Hilbert complexes is to construct finite-dimensional spaces that fit in a complex. These spaces should have certain continuity and inherit algebraic and differential structures on the continuous level, e.g., exactness. Construction of spaces with high regularity is naturally connected with spline theory. In contrast, allowing low regularity often leads to spaces involving Dirac measures, which we will refer to as *distributional finite elements* [19, 27, 54]. The construction of simplicial splines is subtle due to intrinsic supersmoothness [35, 69] (piecewise smooth functions may have automatic higher order continuity at hinges, e.g., vertices and edges of a mesh). The construction of distributional finite elements is usually more straightforward, but numerical schemes call for attention. The general idea is to choose proper combinations of spaces such that Dirac measures are only evaluated on continuous functions or forms [37, 62]. The situation can be more subtle for nonlinear problems since the product of Dirac measures is not defined in general (c.f. [14, 28, 38]).

This report will mainly focus on the construction of conforming finite elements. On cubical meshes, the tensor product provides a useful algebraic tool to derive elements and complexes in any dimension from results in 1D [4, 16, 17]. On simplicies, there are two general strategies to handle supersmoothness: incorporating supersmoothness in the definition of finite element spaces (e.g., the Argyris C^1 element with second order vertex derivative degrees of freedom) or subdividing a simplex and seeking piecewise polynomials on the refined mesh (e.g., the Clough-Tocher C^1 element). In general, several possible constructions exist and finer subdivisions usually require less supersmoothness, c.f. [32, 36, 39, 58].

de-Rham complex. The development of discrete de-Rham complexes demonstrates deep connections between topology and numerical analysis. The Raviart-Thomas [64], Nédélec [56, 57] and Brezzi-Douglas-Marini [20] finite elements achieved success in computational electromagnetism and other areas. It was realized later that these finite elements fit in a discrete de-Rham complex, and the lowest order version coincides with the Whitney forms in geometric integration theory [70]. This observation inspired the development of discrete differential forms [18, 44, 45] and the finite element exterior calculus [3, 6, 7]. The finite element periodic table [9] summarized several families of de-Rham finite elements on simplicial and cubical meshes. Poincaré (Koszul) operators, \mathbf{p}^j , $j = 1, 2, \dots, n$, satisfying $d^{k-1}\mathbf{p}^k + \mathbf{p}^{k+1}d^k = I$, provide explicit forms of potential and thus lead to polynomial exact sequences on cells [6, 44].

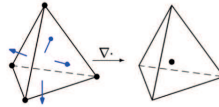
Smoother de-Rham (Stokes) complexes. Stokes problems in fluid mechanics raise the question of constructing a finite element velocity space $V_h \subset [H^1]^3$ and a pressure space $Q_h \subset L^2$ such that $\operatorname{div} V_h = Q_h$ and the inf-sup condition holds.

The Stokes problem motivates discretizing de-Rham complexes that are smoother than the standard $H\Lambda$ version (u in L^2 with du in L^2). On the continuous level, there are several possible combinations of Sobolev spaces that fit in a de-Rham complex, and the following has a direct application in the 2D Stokes problem [34]:

$$0 \longrightarrow H^2 \xrightarrow{\text{curl}} [H^1]^2 \xrightarrow{\text{div}} L^2 \longrightarrow 0.$$

The above sequence shows connections between scalar high order problems (H^2) and the Stokes problem ($\text{div} : [H^1]^2 \rightarrow L^2$). To a large extent, these two topics were developed independently over a long time (see, e.g., [10, 52, 71, 72]) until smoother de-Rham complexes built a bridge. On the one hand, one may differentiate scalar splines and obtain a Stokes pair. On the other hand, investigating the pre-image of the divergence operator helps to clarify the inf-sup stability of Stokes pairs (e.g., the Scott-Vogelius elements [42, 68]).

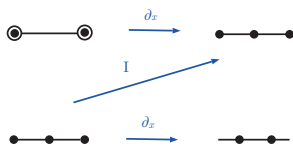
Most existing conforming elements either use subdivision (e.g., [10, 36, 39, 72]) or/and higher order derivatives as degrees of freedom (e.g., [34, 58, 59]), which are two general strategies for handling supersmoothness. Recent development in 2D and 3D can be found in, e.g., [2, 32, 40, 41, 51]. In the direction of reducing the number of degrees of freedom, one is interested in a minimal Stokes pair, where the degrees of freedom for the velocity space involve vertex evaluation (for approximation) and normal component on each face (for surjectivity of div).



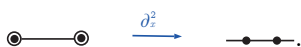
Bernardi and Raugel [15] constructed elements with the above degrees of freedom by enriching Lagrange elements with face bubbles. The resulting elements do not fit in a complex. Guzmán and Neilan [41] modified the bubbles using modes on the Alfeld split of a tetrahedron to render the complex property (see also [51] for the entire complex). A canonical construction on various subdivisions can be found in [32].

BGG complexes. BGG complexes, as well as the BGG diagrams that lead to them, encode structures of many PDE problems [8, 60, 61]. Since the construction of the Arnold-Winther element [11], which was the first conforming triangular finite element with polynomial shape functions, several discretizations for linear elasticity were developed (e.g., [49, 50]). Recently, there has been a surge of finite elements for Hilbert complexes, especially the Hessian, elasticity and div div complexes in 2D and 3D [2, 21, 22, 23, 24, 25, 29, 33, 46, 47, 48, 66].

The approach in [8] for deriving BGG complexes on the continuous level is to collect several copies of de-Rham complexes and eliminate some components. Therefore a natural approach to deriving discrete BGG complexes is to mimic the construction and fit finite element spaces in diagrams. A simple example is demonstrated in the following diagram, where one connects two 1D de-Rham complexes



to derive a finite element complex with a second order differential operator:



This example also demonstrates that the input discrete de-Rham complexes should have different regularity in this approach. Such finite element diagram chasing was first used in [5] as a re-interpretation of the Arnold-Winther elasticity element. Recently, this approach has been extended to derive more complexes with applications in discretizing elasticity and curvature [29, 31, 33].

One may also directly discretize the BGG complexes without referring to the BGG diagrams. Hu and collaborators [46, 47, 48, 49] constructed several conforming finite element complexes in 2D and 3D based on explicit characterizations of bubble functions and an investigation of Lagrange type bases. Chen and Huang [21, 22, 23, 24, 25] further developed geometric decomposition and polynomial BGG complexes and obtained various conforming finite element complexes. There has been progress towards a systematic discretization of BGG complexes in any dimension [16, 22] and a wide variety of continuity [26].

Summary and overlook. This report aims to review some progress on discretizing Hilbert complexes. The emphasis is mainly on conforming finite elements on simplices, while other important topics are not covered, e.g., polygonal elements, virtual elements, isogeometric analysis, nonconforming elements and applications.

Canonical finite element de-Rham complexes have been implemented in several packages, e.g., FEniCS [1], Firedrake [13], NGSolve [67]. Nevertheless, most existing smoother finite element de-Rham (Stokes) complexes and BGG complexes have not been included. An exception is the Regge element. Regge calculus [65] was proposed as a scheme for quantum and numerical gravity, and later interpreted as a finite element [27, 53]. The Regge element has been implemented in several finite element packages [1, 13, 67].

Computational issues, e.g., well-conditioned bases and implementation, remain open, especially for the BGG complexes. Ideas and algorithms for scalar splines may carry over here by complexes. General constructions of distributional and nonconforming elements for the BGG complexes call for further investigation. These elements enjoy simple degrees of freedom, and may thus provide a bridge for discretization of PDEs and discrete structures, including graph theory [55], discrete mechanics [43], discrete differential geometry [14, 27, 33, 38, 53] and gauge theory [30]. Finite elements may provide a new perspective for these areas by supplying local shape functions [27] and inspire new schemes. Recent progress on Hilbert complexes paves a way to tackle the Einstein equations with applications in numerical relativity [12, 53, 63].

REFERENCES

- [1] Alnaes, M., Blechta, J., Hake, J., Johansson, A., Kehlet, B., Logg, A., Richardson, C., Ring, J., Rognes, M. & Wells, G. The FEniCS Project Version 1.5, *Archive of Numerical Software* **3** (2015).
- [2] Arf, J. & Simeon, B. Structure-preserving discretization of the Hessian complex based on spline spaces. *ArXiv Preprint ArXiv:2109.05293*. (2021)
- [3] Arnold, D. Finite element exterior calculus. (SIAM,2018)
- [4] Arnold, D., Boffi, D. & Bonizzoni, F. Finite element differential forms on curvilinear cubic meshes and their approximation properties. *Numerische Mathematik*. **129**, 1-20 (2015)
- [5] Arnold, D., Falk, R. & Winther, R. Differential complexes and stability of finite element methods II: The elasticity complex. *Compatible Spatial Discretizations*. pp. 47-67 (2006)
- [6] Arnold, D., Falk, R. & Winther, R. Finite element exterior calculus, homological techniques, and applications. *Acta Numerica*. **15** pp. 1 (2006)
- [7] Arnold, D., Falk, R. & Winther, R. Finite element exterior calculus: from Hodge theory to numerical stability. *Bulletin Of The American Mathematical Society*. **47**, 281-354 (2010)
- [8] Arnold, D. & Hu, K. Complexes from complexes. *Foundations Of Computational Mathematics*. pp. 1-36 (2021)
- [9] Arnold, D. & Logg, A. Periodic table of the finite elements. *SIAM News*. **47** (2014)
- [10] Arnold, D. & Qin, J. Quadratic velocity/linear pressure Stokes elements. *Advances In Computer Methods For Partial Differential Equations*. **7** pp. 28-34 (1992)
- [11] Arnold, D. & Winther, R. Mixed finite elements for elasticity. *Numerische Mathematik*. **92**, 401-419 (2002)
- [12] Beig, R. & Chruściel, P. On linearised vacuum constraint equations on Einstein manifolds. *Classical and Quantum Gravity*, **37** (2020)
- [13] Bercea, G.-T., McRae, A., Ham, D., Mitchell, L., Rathgeber, F., Nardi, L., Luporini, F. & Kelly, P. A structure-exploiting numbering algorithm for finite elements on extruded meshes, and its performance evaluation in firedrake. *Geoscientific Model Development*, **9**:3803–3815 (2016).
- [14] Berchenko-Kogan, Y. & Gawlik, E. Finite element approximation of the Levi-Civita connection and its curvature in two dimensions. *ArXiv Preprint ArXiv:2111.02512*. (2021)
- [15] Bernardi, C. & Raugel, G. Analysis of some finite elements for the Stokes problem, *Mathematics of Computation*, **44**:71–79 (1985).
- [16] Bonizzoni, F., Hu, K., Kanschat, G. & Sap, D. Spline and finite element BGG complexes on cubical meshes. *In Preparation* (2022)
- [17] Bonizzoni, F. & Kanschat, G. H1-conforming finite element cochain complexes and commuting quasi-interpolation operators on Cartesian meshes. *Calcolo*. **58**, 1-29 (2021)
- [18] Bossavit, A. Whitney forms: A class of finite elements for three-dimensional computations in electromagnetism. *IEE Proceedings A (Physical Science, Measurement And Instrumentation, Management And Education, Reviews)*. **135**, 493-500 (1988)
- [19] Braess, D. & Schöberl, J. Equilibrated residual error estimator for edge elements. *Mathematics Of Computation*. **77**, 651-672 (2008)
- [20] Brezzi, F., Douglas Jr, J. & Marini, L. Two families of mixed finite elements for second order elliptic problems. *Numerische Mathematik*. **47**, 217-235 (1985)
- [21] Chen, L. & Huang, X. Discrete Hessian complexes in three dimensions. In “*The Virtual Element Method and its Applications*”. *SEMA-SIMAI Springer series*. (2021)
- [22] Chen, L. & Huang, X. Finite elements for div- and divdiv-conforming symmetric tensors in arbitrary dimension. *SIAM Journal on Numerical Analysis*. **60**, 1932-1961 (2022)
- [23] Chen, L. & Huang, X. A finite element elasticity complex in three dimensions. *Mathematics of Computation*. **91**, 2095-2127 (2022)
- [24] Chen, L. & Huang, X. Finite elements for divdiv-conforming symmetric tensors in three dimensions. *Mathematics of Computation*. **91**, 1107-1142 (2022)
- [25] Chen, L. & Huang, X. Geometric decompositions of div-conforming finite element tensors. *ArXiv Preprint ArXiv:2112.14351*. (2021)

- [26] Chen, L. & Huang, X. Finite element complexes in two dimensions. *arXiv preprint arXiv:2206.00851*. (2022)
- [27] Christiansen, S. On the linearization of Regge calculus. *Numerische Mathematik*. **119**, 613-640 (2011)
- [28] Christiansen, S. Exact formulas for the approximation of connections and curvature. *ArXiv Preprint ArXiv:1307.3376*. (2013)
- [29] Christiansen, S., Gopalakrishnan, J., Guzman, J. & Hu, K. A discrete elasticity complex on three-dimensional Alfeld splits. *ArXiv Preprint ArXiv:2009.07744*. (2020)
- [30] Christiansen, S. & Halvorsen, T. A simplicial gauge theory. *Journal Of Mathematical Physics*. **53**, 033501 (2012)
- [31] Christiansen, S., Hu, J. & Hu, K. Nodal finite element de Rham complexes. *Numerische Mathematik*. **139**, 411-446 (2018)
- [32] Christiansen, S. & Hu, K. Generalized finite element systems for smooth differential forms and Stokes' problem. *Numerische Mathematik*. **140**, 327-371 (2018)
- [33] Christiansen, S. & Hu, K. Finite element systems for vector bundles: elasticity and curvature. *Foundations Of Computational Mathematics*. pp. 1-52 (2022)
- [34] Falk, R. & Neilan, M. Stokes complexes and the construction of stable finite elements with pointwise mass conservation. *SIAM Journal On Numerical Analysis*. **51**, 1308-1326 (2013)
- [35] Floater, M. & Hu, K. A characterization of supersmoothness of multivariate splines. *Advances In Computational Mathematics*. **46**, 1-15 (2020)
- [36] Fu, G., Guzman, J. & Neilan, M. Exact smooth piecewise polynomial sequences on Alfeld splits. *Mathematics Of Computation*. **89**, 1059-1091 (2020)
- [37] Gopalakrishnan, J., Lederer, P. & Schöberl, J. A mass conserving mixed stress formulation for the Stokes equations. *IMA Journal of Numerical Analysis*. **40**, 1838-1874 (2020)
- [38] Gopalakrishnan, J., Neunteufel, M., Schöberl, J. & Wardetzky, M. Analysis of curvature approximations via covariant curl and incompatibility for Regge metrics. *ArXiv Preprint ArXiv:2206.09343*. (2022)
- [39] Guzman, J., Lischke, A. & Neilan, M. Exact sequences on Worsley–Farin splits. *Mathematics Of Computation*. (2022)
- [40] Guzman, J., Lischke, A. & Neilan, M. Exact sequences on Powell–Sabin splits. *Calcolo*. **57**, 1-25 (2020)
- [41] Guzman, J. & Neilan, M. Inf-sup stable finite elements on barycentric refinements producing divergence-free approximations in arbitrary dimensions. *SIAM Journal On Numerical Analysis*. **56**, 2826-2844 (2018)
- [42] Guzman, J. & Scott, R. The Scott-Vogelius finite elements revisited. *ArXiv Preprint ArXiv:1705.00020*. (2017)
- [43] Hauret, P., Kuhl, E. & Ortiz, M. Diamond elements: a finite element/discrete-mechanics approximation scheme with guaranteed optimal convergence in incompressible elasticity. *International Journal For Numerical Methods In Engineering*. **72**, 253-294 (2007)
- [44] Hiptmair, R. Canonical construction of finite elements. *Mathematics Of Computation Of The American Mathematical Society*. **68**, 1325-1346 (1999)
- [45] Hiptmair, R. Higher order Whitney forms. *Progress In Electromagnetics Research*. **32** pp. 271-299 (2001)
- [46] Hu, J. & Liang, Y. Conforming discrete Gradgrad-complexes in three dimensions. *Mathematics Of Computation*. **90**, 1637-1662 (2021)
- [47] Hu, J., Liang, Y. & Ma, R. Conforming finite element DIVDIV complexes and the application for the linearized Einstein-Bianchi system. *ArXiv Preprint ArXiv:2103.00088*. (2021)
- [48] Hu, J., Liang, Y., Ma, R. & Zhang, M. New conforming finite element divdiv complexes in three dimensions. *ArXiv Preprint ArXiv:2204.07895*. (2022)
- [49] Hu, J. & Zhang, S. A family of symmetric mixed finite elements for linear elasticity on tetrahedral grids. *Science China Mathematics*. **58**, 297-307 (2015)
- [50] Hu, J. & Zhang, S. Finite element approximations of symmetric tensors on simplicial grids in \mathbb{R}^n : the lower order case. *Mathematical Models And Methods In Applied Sciences*. (2016)

- [51] Hu, K., Zhang, Q. & Zhang, Z. A family of finite element Stokes complexes in three dimensions. *SIAM Journal On Numerical Analysis*. **60**, 222-243 (2022)
- [52] Lai, M. & Schumaker, L. Spline functions on triangulations. (Cambridge University Press, 2007)
- [53] Li, L. Regge finite elements with applications in solid mechanics and relativity. (University of Minnesota, 2018)
- [54] Licht, M. Complexes of discrete distributional differential forms and their homology theory. *Foundations Of Computational Mathematics*. **17**, 1085-1122 (2017)
- [55] Lim, L. Hodge Laplacians on graphs. *SIAM Review*. **62**, 685-715 (2020)
- [56] Nédélec, J. Mixed finite elements in \mathbb{R}^3 . *Numerische Mathematik*. **35** pp. 315-341 (1980)
- [57] Nédélec, J. A new family of mixed finite elements in \mathbb{R}^3 . *Numerische Mathematik*. **50** pp. 57-81 (1986)
- [58] Neilan, M. Discrete and conforming smooth de Rham complexes in three dimensions. *Mathematics Of Computation*. (2015)
- [59] Neilan, M. The Stokes complex: A review of exactly divergence-free finite element pairs for incompressible flows. *75 Years Of Mathematics Of Computation: Symposium On Celebrating 75 Years Of Mathematics Of Computation, November 1-3, 2018, The Institute For Computational And Experimental Research In Mathematics (ICERM)*. **754** pp. 141 (2020)
- [60] Pauly, D. & Zulehner, W. The divDiv-complex and applications to biharmonic equations. *Applicable Analysis*. **99** pp. 1579-1630 (2020)
- [61] Pauly, D. & Zulehner, W. The elasticity complex: compact embeddings and regular decompositions. *ArXiv Preprint ArXiv:2001.11007*. (2020)
- [62] Pechstein, A. & Schöberl, J. Tangential-displacement and normal-normal-stress continuous mixed finite elements for elasticity. *Mathematical Models And Methods In Applied Sciences*. **21**, 1761-1782 (2011)
- [63] Quenneville-Belair, V. A new approach to finite element simulations of general relativity. (University of Minnesota, 2015).
- [64] Raviart, P. & Thomas, J. A mixed finite element method for second order elliptic problems. *Lecture Notes In Mathematics*. **606** pp. 292-315 (1977)
- [65] Regge, T. General relativity without coordinates. *Il Nuovo Cimento (1955-1965)*. pp. 558-571 (1961)
- [66] Sander, O. Conforming finite elements for $H(\text{sym curl})$ and $H(\text{dev sym curl})$. *ArXiv Preprint ArXiv:2104.12825*. (2021)
- [67] Schöberl, J. C++11 implementation of finite elements in NGSolve (2014)
- [68] Scott, L. & Vogelius, M. Norm estimates for a maximal right inverse of the divergence operator in spaces of piecewise polynomials. *ESAIM: Mathematical Modelling And Numerical Analysis*. **19**, 111-143 (1985)
- [69] Sorokina, T. Intrinsic supersmoothness of multivariate splines. *Numerische Mathematik*. **116**, 421-434 (2010)
- [70] Whitney, H. Geometric integration theory. (Courier Corporation, 2012)
- [71] Zhang, S. A new family of stable mixed finite elements for the 3D Stokes equations. *Mathematics Of Computation*. **74**, 543-554 (2005)
- [72] Zhang, S. On the P1 Powell-Sabin divergence-free finite element for the Stokes equations. *Journal Of Computational Mathematics*. pp. 456-470 (2008)

Finite element systems

SNORRE H. CHRISTIANSEN

Recall the definition of a finite element by Ciarlet. It consists of three parts: A geometric cell T (for instance a simplex), a space $A(T)$ of fields on T (for instance vector fields that are polynomial, with given maximum degree), and a set of degrees of freedom that are unisolvent on $A(T)$. We point out some shortcomings of the definition, by expressing what is implicit: First, degrees of freedom are geometrically located (attached to subcells of T). Second, there is a way of identifying degrees of freedom attached to a subcell, from incident cells.

The framework of finite element systems addresses these problems by positing instead the following. A finite element is defined given a cellular complex \mathcal{T} . Then it is a contravariant functor A from \mathcal{T} (interpreted as a poset category) to the category of vector spaces.

This definition expresses that there are in fact spaces attached to cells of all dimensions in \mathcal{T} , and that they are linked by restriction maps, satisfying obvious commutation relations.

I gave some examples of known finite element systems: trimmed polynomial differential forms, the Clough-Tocher element, the Argyris element, the Morley element. For the last three spaces the only difficulty is to come up with the spaces attached to edges. The claim is that all nice finite elements can be recast as finite element systems, and that this point of view reveals some useful facts.

The global finite element space is then deduced as an inverse limit. The global space will not always be a good space: the continuity requirement inherent in taking the inverse limit can result in global linear dependencies, preventing local bases. To avoid such rigidity properties we introduce a notion of softness. It is related on the one hand to the unisolvence in Ciarlet's definition of a FE and on the other hand to softness of sheaves. Several characterizations of softness are possible, e.g. with dimension counts.

Given two finite element systems – two functors – one can consider the natural transformations from one to the other. These are linear maps that commute with the restriction maps. Differential operators, inclusion maps, and interpolation operators are all examples of natural transformations.

When we have sequences of soft finite element systems, linked by differential operators that are natural transformations and form complexes, the global spaces are also complexes. Importantly, the cohomology of the global spaces is the right one: it is isomorphic to the cellular cochain cohomology. This is a variant of de Rham's theorem.

The framework works both for spaces of differential forms [1] (here we introduced spaces with enhanced continuity, such as appears in Stokes problem) and for complexes appearing in elasticity or Riemannian geometry [2]. In the latter case cochains with values in rigid motions play a special role.

REFERENCES

- [1] S. H. Christiansen, K. Hu, *Generalized Finite Element Systems for smooth differential forms and Stokes' problem*, Numer. Math., Vol. 140, No. 2, p. 327–371, 2018.
- [2] S. H. Christiansen, K. Hu, *Finite Element Systems for vector bundles: elasticity and curvature*, Found. Comput. Math., 2022.

Finite elements for Riemannian geometry

EVAN S. GAWLIK

(joint work with Yakov Berchenko-Kogan)

The building blocks of Riemannian geometry – metrics, connections, and curvature – play an important role in mathematical physics and geometric analysis, but they are challenging to discretize numerically. Here we discuss recent efforts to discretize these objects with finite elements. Many of these efforts are guided by commutative diagrams of differential complexes.

Given a triangulation \mathcal{S} of a compact, oriented manifold of dimension N , the lengths of all of the edges in \mathcal{S} determine a piecewise constant Riemannian metric g on \mathcal{S} . This metric automatically possesses the following continuity property: g has single-valued tangential-tangential components on every $(N - 1)$ -dimensional simplex in \mathcal{S} . The metric g is an example of a tensor field belonging to the lowest-order *Regge finite element space* Σ_h^0 [3, 6], a space that has been studied extensively and generalized to higher order in the thesis of Li [6]. For an integer $r \geq 0$, the Regge finite element space Σ_h^r of order r consists of symmetric $(0, 2)$ -tensor fields on \mathcal{S} that are piecewise polynomial of degree at most r and obey the same tangential-tangential continuity constraint as above. We call elements of this space *Regge metrics* if they are positive definite everywhere.

Although Regge metrics cannot be differentiated in the classical sense, one can give meaning to a Regge metric's scalar curvature (times the volume form ω) in a distributional sense. In dimension $N = 2$, one defines the distributional curvature two-form $(\kappa\omega)_{\text{dist}}(g)$ associated with a Regge metric g as follows. Let \mathcal{V} , \mathcal{E} , and \mathcal{T} denote the set of vertices, edges, and triangles in \mathcal{S} , and assume that \mathcal{S} has no boundary. Let V be the space of continuous functions whose restrictions to each triangle $T \in \mathcal{T}$ lie in the Sobolev space $H^2(T)$. We define $(\kappa\omega)_{\text{dist}}(g) \in V'$ via

$$\langle (\kappa\omega)_{\text{dist}}(g), v \rangle_{V', V} = \sum_{T \in \mathcal{T}} \int_T \kappa_T v \omega_T + \sum_{e \in \mathcal{E}} \int_e \llbracket k \rrbracket_e v \omega_e + \sum_{z \in \mathcal{V}} \Theta_z v(z), \quad \forall v \in V,$$

where κ_T is the (classically defined) Gaussian curvature of g within the triangle T , ω_T is the volume form on T , ω_e is the induced length form on e , $\llbracket k \rrbracket_e$ denotes the jump in e 's geodesic curvature across e , and Θ_z is the *angle defect* at the vertex z : 2π minus the sum of the angles incident at z (as measured by g).

It turns out that a great deal of information about a Regge metric's distributional curvature can be gleaned from studying its evolution under deformations of the metric. For one thing, doing so allows us to show that the distributional curvature operator described above is (infinitesimally) consistent; its linearization

around a given Regge metric g is precisely the linearized curvature operator, interpreted in a distributional sense. In particular, we show in [1, Theorem 4.1] that if $g(t)$ is a family of Regge metrics with $\frac{\partial}{\partial t}g =: \sigma$, then for every $v \in V$,

$$(1) \quad 2 \frac{d}{dt} \langle (\kappa\omega)_{\text{dist}}(g(t)), v \rangle_{V',V} = \sum_{T \in \mathcal{T}} \int_T \langle \mathbb{S}\sigma, \nabla \nabla v \rangle \omega_T - \sum_{e \in \mathcal{E}} \int_e \mathbb{S}\sigma(n, n) [\nabla_n v] \omega_e.$$

Here, $\mathbb{S}\sigma = \sigma - g \text{Tr} \sigma$, ∇ is the covariant derivative, n is the unit normal vector to e with respect to g , and $\langle \cdot, \cdot \rangle$ is the g -inner product of tensor fields.

Numerical analysts will recognize the right-hand side of (1); its Euclidean counterpart appears in the Hellan-Herrmann-Johnson (HHJ) finite element discretization of $\int (\text{div div } \mathbb{S}\sigma)v\omega$. This link with the HHJ method naturally leads one to consider using the Regge finite element space Σ_h^r to discretize the metric tensor and the Lagrange finite element space $V_h^q = \{v \in V \mid v|_T \in \mathcal{P}_q(T), \forall T \in \mathcal{T}\}$, $q \geq 1$, to discretize the scalar curvature in two dimensions. One defines a discrete scalar curvature $\kappa_h \in V_h^q$ via $\int \kappa_h v_h \omega = \langle (\kappa\omega)_{\text{dist}}(g), v_h \rangle_{V',V}$ for every $v_h \in V_h^q$. If $g_h \in \Sigma_h^r$ is an interpolant of a smooth Riemannian metric g on a planar domain Ω , then an error estimate

$$\|\kappa_h(g_h) - \kappa(g)\|_{H^{-1}(\Omega)} \leq C (h^r |g|_{H^{r+1}(\Omega)} + h^{q+2} |\kappa(g)|_{H^{q+1}(\Omega)})$$

can be proved [4, Theorem 4.1] by exploiting the fact that the smooth curvature $\kappa(g)$ and its discretization $\kappa_h(g_h)$ both satisfy an equality of the form (1), albeit with different metrics on the right-hand side. Here, $h = \max_{T \in \mathcal{T}} \text{diam}(T)$. A sharper estimate has recently been proven in the case where $q = r + 1$ and g_h is the canonical Regge interpolant of g [5].

When g and g_h are Euclidean and $q = r + 1$, the spaces above fit into a commutative diagram of differential complexes which is discussed in [1, Section 7.1]:

$$\begin{CD} RM @>C>> U @>{\text{def}}>> \Sigma @>{(\text{div div } \mathbb{S})_{\text{dist}}}>> V' @>> 0 \\ @. @V{\pi_h^U}VV @V{\pi_h^\Sigma}VV @V{\pi_h^V}VV \\ RM @>C>> U_h^{r+1} @>{\text{def}}>> \Sigma_h^r @>{(\text{div div } \mathbb{S})_h}>> V_h^{r+1} @>> 0 \end{CD}$$

This diagram is related to ones that appear in [3, 2]. Briefly, the space U_h^{r+1} consists of continuous vector fields that are piecewise polynomial of degree $r + 1$, RM consists of the rigid motions, U and Σ are certain infinite-dimensional superspaces of U_h^{r+1} and Σ_h^r , def is the symmetric gradient, $(\text{div div } \mathbb{S})_{\text{dist}}$ is the distributional linearized curvature operator, and $(\text{div div } \mathbb{S})_h$ is its discrete counterpart.

In dimension $N > 2$, preliminary work suggests that the distributional scalar curvature (times the volume form) of a Regge metric g becomes

$$\langle (R\omega)_{\text{dist}}(g), v \rangle_{V',V} = \sum_T \int_T R_T v \omega_T + 2 \sum_F \int_F \llbracket H \rrbracket_F v \omega_F + 2 \sum_S \int_S \Theta_S v \omega_S, \forall v \in V,$$

where the first sum is over N -simplices T , the second is over $(N - 1)$ -simplices F , and the third is over $(N - 2)$ -simplices S . Here, R_T denotes the (classically defined) scalar curvature of g within T (which equals $2\kappa_T$ in dimension $N = 2$),

$[[H]]_F$ denotes the jump in F 's mean curvature across F , and Θ_S denotes the angle defect along S , which may vary along S .

If $g(t)$ is a family of Regge metrics in dimension N with $\frac{\partial}{\partial t}g =: \sigma$, then one finds

$$(2) \quad \begin{aligned} \frac{d}{dt} \langle (R\omega)_{\text{dist}}(g(t)), v \rangle_{V',V} &= \sum_T \int_T \langle \mathbb{S}\sigma, \nabla \nabla v \rangle \omega_T - \sum_F \int_F \mathbb{S}\sigma(n, n) [[\nabla_n v]] \omega_F \\ &- \sum_T \int_T \langle G, \sigma \rangle v \omega_T - \sum_F \int_F \langle [[\mathbb{I}]], \sigma|_F \rangle v \omega_F + \sum_S \int_S \Theta_S \text{Tr}(\sigma|_S) v \omega_S, \end{aligned}$$

where $G = \text{Ric} - \frac{1}{2}Rg$ denotes the Einstein tensor, and $\mathbb{I}(X, Y) = g(\nabla_X n, Y) - Hg(X, Y)$ is the trace-reversed second fundamental form on F . We recognize (2) as a distributional version of the identity

$$\frac{d}{dt} \int Rv\omega = \int (\text{div div } \mathbb{S}\sigma)v\omega - \int \langle G, \sigma \rangle v\omega$$

that holds in the smooth setting. The appearance of $[[\mathbb{I}]]$ lends credence to this assertion; the same quantity arises in studies of singular sources in general relativity, where it encodes the so-called *Israel junction conditions* across a hypersurface [7].¹

This motivates the following definition. Given a Regge metric g , the *discrete Einstein tensor* G_h associated with g is the unique element of Σ_h^r satisfying

$$(3) \quad \int \langle G_h, \sigma_h \rangle \omega = \sum_T \int_T \langle G, \sigma_h \rangle \omega_T + \sum_F \int_F \langle [[\mathbb{I}]], \sigma_h|_F \rangle \omega_F - \sum_S \int_S \Theta_S \text{Tr}(\sigma_h|_S) \omega_S$$

for every $\sigma_h \in \Sigma_h^r$. In dimension $N = 2$, one can check that the right-hand side of (3) simplifies to zero, which is consistent with the fact that the Einstein tensor always vanishes in two dimensions. In N dimensions, our preliminary numerical experiments suggest that (3) yields a G_h that converges in a weak sense to its smooth counterpart under refinement of the triangulation; analysis is ongoing.

REFERENCES

- [1] Y. Berchenko-Kogan and E. S. Gawlik, *Finite element approximation of the Levi-Civita connection and its curvature in two dimensions*, arXiv preprint 2111.02512 (2021).
- [2] L. Chen, J. Hu, and X. Huang, *Multigrid methods for Hellan–Herrmann–Johnson mixed method of Kirchhoff plate bending problems*, *Journal of Scientific Computing* **76**(2) (2018), 673–696.
- [3] S. H. Christiansen, *On the linearization of Regge calculus*, *Numerische Mathematik* **119**(4) (2011), 613–640.
- [4] E. S. Gawlik, *High-order approximation of Gaussian curvature with Regge finite elements*, *SIAM Journal on Numerical Analysis* **58**(3) (2020), 1801–1821.
- [5] J. Gopalakrishnan, M. Neunteufel, J. Schöberl, and M. Wardetzky, *Analysis of curvature approximations via covariant curl and incompatibility for Regge metrics*, arXiv preprint 2206.09343 (2022).

¹Thanks to Snorre Christiansen for pointing out this connection.

- [6] L. Li, *Regge finite elements with applications in solid mechanics and relativity*, PhD thesis, University of Minnesota (2018).
- [7] W. Israel, *Singular hypersurfaces and thin shells in general relativity*, Il Nuovo Cimento B (1965-1970), **44**(1) (1966), 1–14.

Smooth finite element sequences on Worsley-Farin splits

MICHAEL NEILAN

(joint work with Johnny Guzmán, Anna Lischke)

Motivated by structure-preserving and divergence-free discretizations of incompressible flow, we construct various Stokes complexes, consisting of piecewise polynomial spaces, with respect to three-dimensional simplicial triangulations. In particular, we consider the following de Rham complexes with enhanced regularity:

$$\begin{aligned} \mathbb{R} &\longrightarrow H^2(\Omega) \xrightarrow{\text{grad}} H^1(\text{curl}; \Omega) \xrightarrow{\text{curl}} [H^1(\Omega)]^3 \xrightarrow{\text{div}} L^2(\Omega) \longrightarrow 0, \\ \mathbb{R} &\longrightarrow H^2(\Omega) \xrightarrow{\text{grad}} H^1(\text{curl}; \Omega) \xrightarrow{\text{curl}} H^1(\text{div}; \Omega) \xrightarrow{\text{div}} H^1(\Omega) \longrightarrow 0, \end{aligned}$$

to construct discrete analogues:

$$(1) \quad \begin{aligned} \mathbb{R} &\longrightarrow \mathcal{S}_h^0 \xrightarrow{\text{grad}} \mathcal{S}_h^1 \xrightarrow{\text{curl}} \mathcal{L}_h^2 \xrightarrow{\text{div}} \mathcal{V}_h^3 \longrightarrow 0, \\ \mathbb{R} &\longrightarrow \mathcal{S}_h^0 \xrightarrow{\text{grad}} \mathcal{S}_h^1 \xrightarrow{\text{curl}} \mathcal{S}_h^2 \xrightarrow{\text{div}} \mathcal{L}_h^3 \longrightarrow 0, \end{aligned}$$

where $\mathcal{S}_h^0 \subset H^2(\Omega)$, $\mathcal{S}_h^1 \subset H^1(\text{curl}; \Omega)$, $\mathcal{S}_h^2 \subset H^1(\text{div}; \Omega)$, $\mathcal{L}_h^2 \subset [H^1(\Omega)]^3$, $\mathcal{L}_h^3 \subset H^1(\Omega)$, and $\mathcal{V}_h^3 \subset L^2(\Omega)$ are finite dimensional spaces consisting of piecewise polynomials with respect to a simplicial mesh of Ω . The last two (non-trivial) spaces in the sequences may be suitable for discretizations for incompressible flows. Provided the discrete complexes (1) are exact, and if the mapping $\text{div} : \mathcal{L}_h^2 \rightarrow \mathcal{V}_h^3$ (resp., $\text{div} : \mathcal{S}_h^2 \rightarrow \mathcal{L}_h^3$) has a bounded right-inverse, then the pair $\mathcal{L}_h^2 \times \mathcal{V}_h^3$ (resp., $\mathcal{S}_h^2 \times \mathcal{L}_h^3$) constitutes a stable and divergence-free for the Stokes/NSE problem. This framework also indicates a connection between H^2 -conforming finite element spaces and divergence-free pairs.

On general simplicial triangulations, conforming H^2 -spaces finite element spaces require high polynomial degree and complexity. For example, on general three-dimensional simplicial meshes, H^2 -conforming spaces require polynomial degrees of at least nine. In addition, such spaces have extrinsic supersmoothness (e.g., constrained to be C^4 at vertices and C^2 on edges). The relationships between distinct finite element spaces in (1) imply many of these attributes of smooth finite element spaces translate to divergence-free pairs.

To reduce the complexity and polynomial degree of the discrete spaces, we consider discrete complexes (1) defined on splits of simplicial triangulations, in particular, Worsley-Farin (WF) splits. On such splits, there exists H^2 -conforming finite element spaces (with local bases) of degree three and greater. In addition, these spaces do not possess extrinsic supersmoothness, as their degrees of freedom only involve function and derivative information [3].

Given a simplicial, three-dimensional triangulation \mathcal{T}_h , its WF split \mathcal{T}_h^{wf} is created in three steps: (i) Adjoin the incenter of each $T \in \mathcal{T}_h$ to its vertices; (ii) Connect the incenters of each adjacent pair of tetrahedra with a line segment. This line segment intersects the common face F at a point call m_F ; (iii) Connect m_F to the three vertices of F . Thus, a WF split divides each tetrahedron in the mesh into 12 sub-tetrahdra.

Our first main result concerns exactness properties of discrete spaces defined on a single macro element. Let $T \in \mathcal{T}_h$ be a tetrahedron, and denote by T^{wf} its induced WF refinement consisting of 12 sub-tetrahedra. Let $\mathcal{P}_\ell(T^{wf})$ be the space of (discontinuous) piecewise polynomial of degree $\leq \ell$ with respect to T^{wf} , and set $\mathcal{S}_\ell^0(T^{wf}) = \mathcal{P}_\ell(T^{wf}) \cap \mathring{H}^2(T)$, $\mathcal{S}_\ell^1(T^{wf}) = [\mathcal{P}_\ell(T^{wf})]^3 \cap \mathring{H}^1(\text{curl}; T)$, and $\mathcal{S}_\ell^2(T^{wf}) = [\mathcal{P}_\ell(T^{wf})]^3 \cap \mathring{H}^1(\text{div}; T)$. We further denote $\mathcal{L}_\ell^2(T^{wf}) = [\mathcal{P}_\ell(T^{wf}) \cap \mathring{H}^1(T)]^3$ and $\mathcal{L}_\ell^3(T^{wf}) = \mathcal{P}_\ell(T^{wf}) \cap \mathring{H}^1(T) \cap \mathring{L}^2(T)$ to be the vector and scalar Lagrange spaces, respectively. Then the following sequences are complexes and are exact for $r \geq 3$ [2]:

$$(2) \quad \begin{array}{ccccccc} 0 & \longrightarrow & \mathring{\mathcal{S}}_r^0(T^{wf}) & \xrightarrow{\text{grad}} & \mathring{\mathcal{S}}_{r-1}^1(T^{wf}) & \xrightarrow{\text{curl}} & \mathring{\mathcal{L}}_{r-2}^2(T^{wf}) & \xrightarrow{\text{div}} & \mathring{\mathcal{N}}_{r-3}^3(T^{wf}) & \longrightarrow & 0, \\ 0 & \longrightarrow & \mathring{\mathcal{S}}_r^0(T^{wf}) & \xrightarrow{\text{grad}} & \mathring{\mathcal{S}}_{r-1}^1(T^{wf}) & \xrightarrow{\text{curl}} & \mathring{\mathcal{S}}_{r-2}^2(T^{wf}) & \xrightarrow{\text{div}} & \mathring{\mathcal{L}}_{r-3}^3(T^{wf}) & \longrightarrow & 0. \end{array}$$

Here, $\mathring{\mathcal{N}}_{r-3}^3(T^{wf}) \subset \mathring{H}(\text{curl}; T) \cap [\mathcal{P}_{r-3}(T^{wf})]^3$ is a Nédélec-type space with additional normal continuity at some edges in T^{wf} .

Our second result is a global analogue of (2). For brevity, we describe the global version of the first sequence in (2). To this end, we let $\mathcal{P}_\ell(\mathcal{T}_h^{wf})$ denote the space of piecewise polynomials with respect to the globally refined WF mesh. Set $\mathcal{S}_\ell^0(\mathcal{T}_h^{wf}) = \mathcal{P}_\ell(\mathcal{T}_h^{wf}) \cap H^2(\Omega)$, $\mathcal{S}_\ell^1(\mathcal{T}_h^{wf}) = [\mathcal{P}_\ell(\mathcal{T}_h^{wf})]^3 \cap H^1(\text{curl}; \Omega)$, and $\mathcal{L}_\ell^2(\mathcal{T}_h^{wf}) = [\mathcal{P}_\ell(\mathcal{T}_h^{wf}) \cap H^1(\Omega)]^3$. We further let $\mathcal{N}_\ell(\mathcal{T}_h^{wf})$ be the space of piecewise polynomials with respect to \mathcal{T}_h^{wf} of degree $\leq \ell$ that have an alternating weak continuity property at singular edges (cf. [2]). Then, for $r \geq 3$, there exists operators $\Pi_0 : C^\infty(\Omega) \rightarrow \mathcal{S}_r^0(\mathcal{T}_h)$, $\Pi_1 : [C^\infty(\Omega)]^3 \rightarrow \mathcal{S}_r^1(\mathcal{T}_h)$, $\Pi_2 : [C^\infty(\Omega)]^3 \rightarrow \mathcal{L}_r^2(\mathcal{T}_h)$, and $\Pi_3 : C^\infty(\Omega) \rightarrow \mathcal{N}_r^3(\mathcal{T}_h)$ satisfying the commuting properties

$$\text{grad } \Pi_0 \omega_0 = \Pi_1 \text{grad } \omega_0, \quad \text{curl } \Pi_1 \omega_1 = \Pi_2 \text{curl } \omega_1, \quad \text{div } \Pi_2 \omega_2 = \Pi_3 \text{div } \omega_2.$$

The operators Π_2 and Π_3 can be modified to construct stable Fortin-like operators, resulting in a stable and divergence-free $P_1 - P_0$ discretization for the Stokes problem [1].

REFERENCES

[1] M. Fabien, J. Guzmán, M. Neilan, and A. Zytoon, *Low-order divergence-free approximations for the Stokes problem on Worsey-Farin and Powell-Sabin splits*, *Comput. Methods Appl. Mech. Engrg.* **390** (2022) 114444.
 [2] J. Guzmán, A. Lischke, and M. Neilan, *Exact sequences on Worsey-Farin splits*, *Math. Comp.*, to appear.
 [3] A.J. Worsey and G. Farin, *An n-dimensional Clough-Tocher interpolant*, *Constr. Approx.* **3** (1987), 99–110.

Traces for Hilbert Complexes

RALF HIPTMAIR

(joint work with Dirk Pauly and Erick Schulz)

Motivation. For the 3D Euclidean de Rham complex on a Lipschitz domain $\Omega \subset \mathbb{R}^3$ the trace operators γ (point trace), γ_t (tangential component trace), and γ_n (normal component trace) connect it to a Hilbert complex of functions on the boundary $\Gamma := \partial\Omega$:

$$\begin{array}{ccccccc} H^1(\Omega) \subset L^2(\Omega) & \xrightarrow{\text{grad}} & \mathbf{H}(\text{curl}, \Omega) \subset L^2(\Omega) & \xrightarrow{\text{curl}} & \mathbf{H}(\text{div}, \Omega) \subset L^2(\Omega) & \xrightarrow{\text{div}} & L^2(\Omega) \\ \downarrow \gamma & & \downarrow \gamma_t & & \downarrow \gamma_n & & \\ H^{\frac{1}{2}}(\Gamma) \subset H^{-\frac{1}{2}}(\Gamma) & \xrightarrow{\text{grad}_\Gamma} & \mathbf{H}_\perp^{-\frac{1}{2}}(\text{curl}_\Gamma, \Gamma) \subset \mathbf{H}_\perp^{-\frac{1}{2}}(\Gamma) & \xrightarrow{\text{curl}_\Gamma} & H^{-\frac{1}{2}}(\Gamma) \subset H^{-\frac{1}{2}}(\Gamma) & \xrightarrow{0} & 0, \end{array}$$

where the trace spaces are defined as

$$\begin{aligned} H^{\frac{1}{2}}(\Gamma) &:= \left\{ v \in H^{-\frac{1}{2}}(\Gamma) : \text{grad}_\Gamma v \in \mathbf{H}_\perp^{-\frac{1}{2}}(\Gamma) \right\}, & \mathbf{H}_\perp^{\frac{1}{2}}(\Gamma) &:= \gamma_\times \mathbf{H}^1(\Omega), \\ \mathbf{H}_\perp^{-\frac{1}{2}}(\text{curl}_\Gamma, \Gamma) &:= \left\{ \mathbf{v} \in \mathbf{H}_\perp^{-\frac{1}{2}}(\Gamma) : \text{curl}_\Gamma \mathbf{v} \in H^{-\frac{1}{2}}(\Gamma) \right\}, & \mathbf{H}_\perp^{-\frac{1}{2}}(\Gamma) &:= \left(\mathbf{H}_\perp^{\frac{1}{2}}(\Gamma) \right)', \\ H^{-\frac{1}{2}}(\Gamma) &:= \left\{ v \in H^{-\frac{1}{2}}(\Gamma) \right\}, \end{aligned}$$

Obviously, the trace complex is a Hilbert complex of unbounded surface differential operators based on duals of trace spaces of H^1 -regular functions on Ω . The question is, whether this is a peculiarity of the de Rham complex, or a general structure inherent in a certain class of Hilbert complexes.

Functional traces. Let $\mathbf{W}_k, k \in \mathbb{Z}$, be a sequence of Hilbert spaces, and $A_k : \mathcal{D}(A_k) \subset \mathbf{W}_k \rightarrow \mathbf{W}_{k+1}$, unbounded, closed, densely defined, linear (cddl) operators, satisfying the complex property $A_{k+1} \circ A_k = 0$. In addition, we take for granted another sequence of cddl operators $\mathring{A}_k : \mathcal{D}(\mathring{A}_k) \subset \mathbf{W}_k \rightarrow \mathbf{W}_{k+1}$ with $\mathring{A}_{k+1} \circ \mathring{A}_k = 0$ and $\mathring{A}_k \subset A_k$, that is, $\mathcal{D}(\mathring{A}_k) \subset \mathcal{D}(A_k)$ and $A_k|_{\mathcal{D}(\mathring{A}_k)} = \mathring{A}_k$. This defines a complex and a sub-complex. So do the adjoint operators A_k^* and $A_k^\top := \mathring{A}_k^*$, related by $A_k^* \subset A_k^\top$.

Taking the cue from a generalization of the integration by parts formula we first define the trace in a weak sense.

Definition 1 ((Primal) Hilbert trace, [2, Def. 3.1]). *The primal Hilbert trace $T_k^t : \mathcal{D}(A_k) \rightarrow \mathcal{D}(A_k^\top)'$ is defined by*

$$\langle T_k^t \mathbf{x}, \mathbf{y} \rangle_{\mathcal{D}(A_k^\top)'} := (A_k \mathbf{x}, \mathbf{y})_{\mathbf{W}_{k+1}} - \left(\mathbf{x}, A_k^\top \mathbf{y} \right)_{\mathbf{W}_k} \quad \forall \mathbf{x} \in \mathcal{D}(A_k), \mathbf{y} \in \mathcal{D}(A_k^\top).$$

We find $\|T_k^t\| = 1$ and the kernel $\mathcal{N}(T_k^t) = \mathcal{D}(\mathring{A}_k)$. The range of this trace operator allows a non-trivial characterization.

Theorem 2 (Characterization of “trace space”, [2, Prop. 3.4]).

$$\mathcal{R}(T_k^t) = \mathcal{D}(A_k^*)^\circ := \left\{ \phi \in \mathcal{D}(A_k^\top)' \mid \langle \phi, \mathbf{y} \rangle_{\mathcal{D}(A_k^\top)'} = 0 \quad \forall \mathbf{y} \in \mathcal{D}(A_k^*) \right\}.$$

Quotient traces. For the de Rham complex the trace operators γ , γ_t , and γ_n map onto the corresponding trace spaces, which paves the way for their characterization as quotient spaces. This carries over to the abstract setting.

Theorem 3 (Trace space = quotient space, [2, Thm. 3.10]).

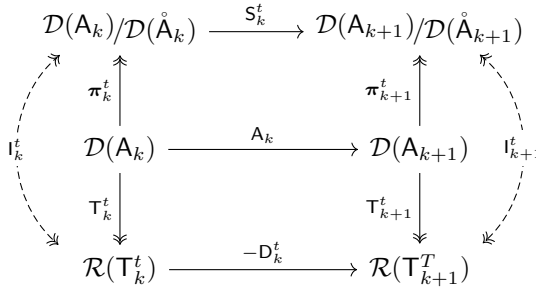
$$I_k^t : \begin{cases} \mathcal{D}(A_k)/\mathcal{D}(\mathring{A}_k) & \rightarrow \mathcal{R}(T_k^t) = \mathcal{D}(A_k^*)^\circ \\ [x] & \mapsto T_k^t x \end{cases} \quad \text{is an isometric isomorphism.}$$

Surface differential operators. Writing $\pi_k^t : \mathcal{D}(A_k) \rightarrow \mathcal{D}(A_k)/\mathcal{D}(\mathring{A}_k)$ for the canonical projections, we can introduce operators mapping between “trace spaces”,

$$D_k^t := (A_{k+1}^\top)' : \mathcal{D}(A_k^\top)' \rightarrow \mathcal{D}(A_{k+1}^\top)',$$

$$S_k^t := \pi_{k+1}^t \circ A_k \circ (\pi_k^t)^{-1} : \mathcal{D}(A_k)/\mathcal{D}(\mathring{A}_k) \rightarrow \mathcal{D}(A_{k+1})/\mathcal{D}(\mathring{A}_{k+1}),$$

which make the following diagram commute:



These are generalized versions of the surface difference operators of the trace De Rham complex.

Characterization of trace spaces. A more detailed characterization of trace space will rely on them, but also on a somewhat extended framework providing so-called regular decompositions:

- We have “more regular” Hilbert spaces $\mathbf{W}_k^+ \subset \mathbf{W}_k$, $k \in \mathbb{Z}$, with *continuous* and *dense embeddings* $\mathbf{W}_k^+ \hookrightarrow \mathcal{D}(A_{k-1}^\top)$.
- There exist *bounded* linear operators

$$L_{k+1}^t : \mathcal{D}(A_k^\top) \rightarrow \mathbf{W}_{k+1}^+ \quad \text{and} \quad V_{k+1}^t : \mathcal{D}(A_k^\top) \rightarrow \mathbf{W}_{k+2}^+$$

such that $\mathbf{y} = (L_{k+1} + A_{k+1}^T V_{k+1}^t) \mathbf{y} \quad \forall \mathbf{y} \in \mathcal{D}(A_k^\top)$.

- The embedding $\mathbf{W}_k^+(A_{k-1}^\top) := \{\mathbf{z} \in \mathbf{W}_k^+ : A_{k-1}^\top \mathbf{z} \in \mathbf{W}_{k-1}^+\} \hookrightarrow \mathcal{D}(A_{k-1}^\top)$ is *continuous* and *dense*.
- The inclusion $\mathbf{W}_k^+ \subset \mathcal{D}(A_{k-1}^\top)$ induces a *continuous* and *dense* embedding $\mathring{\mathbf{W}}_k^+ := \mathbf{W}_k^+ \cap \mathcal{D}(A_{k-1}^*) \hookrightarrow \mathcal{D}(A_{k-1}^*)$.

We point out that the existence of regular decompositions has been verified for a large range of important Hilbert complexes obtained from the de Rham complex by the BGG construction [1, Thm. 3].

Theorem 4 (Characterization of functional trace space, [2, Thm. 6.8]). *Introducing the annihilator $(\mathring{\mathbf{W}}_{k+1}^+)^{\circ} := \{\phi \in \mathbf{W}_{k+1}^- : \langle \phi, \mathbf{y} \rangle_{\mathbf{W}_{k+1}^-} = 0 \ \forall \mathbf{y} \in \mathring{\mathbf{W}}_{k+1}^+\}$, we have*

$$\mathcal{R}(\mathbb{T}_k^t) = \{\psi \in (\mathring{\mathbf{W}}_{k+1}^+)^{\circ} : D_k^t \psi \in (\mathring{\mathbf{W}}_{k+2}^+)^{\circ}\} \quad \text{with equivalent norms.}$$

This induces a similar characterization of quotient trace spaces: [2, Thm. 6.11]:

$$\begin{array}{ccc} \mathcal{R}(\mathbb{T}_k^t) & \cong & \{\psi \in (\mathring{\mathbf{W}}_{k+1}^+)^{\circ} : D_k^t \psi \in (\mathring{\mathbf{W}}_{k+2}^+)^{\circ}\} \\ \updownarrow & & \updownarrow \\ \mathcal{D}(\mathbf{A}_k)/\mathcal{D}(\mathring{\mathbf{A}}_k) & \cong & \{\phi \in (\mathbf{W}_{k+1}^+/\mathring{\mathbf{W}}_{k+1}^+)^{\prime} : (S_{k+1}^n)^{\prime} \phi \in (\mathbf{W}_{k+2}^+/\mathring{\mathbf{W}}_{k+2}^+)^{\prime}\}. \end{array}$$

Note that for the de Rham Hilbert complex the natural choices for \mathbf{W}_k^+ are H^1 -regular functions/vector fields. Then $\mathbf{W}_{k+1}^+/\mathring{\mathbf{W}}_{k+1}^+$ can be identified with suitable dual spaces $H_{\bullet}^{-\frac{1}{2}}(\Gamma)$ and we recover the characterization of the trace spaces $H^{\frac{1}{2}}(\Gamma)$, $H_{\perp}^{-\frac{1}{2}}(\text{curl}_{\Gamma}, \Gamma)$, and $H^{-\frac{1}{2}}(\Gamma)$ given above.

Trace Hilbert complex. The generalized surface differential operators map between trace spaces and spawn a trace Hilbert complex:

Theorem 5 (Trace Hilbert complex, [2, Thm. 7.1]). *The sequence of unbounded operators*

$$\dots \xrightarrow{D_{k-1}^t} \mathcal{R}(\mathbb{T}_k^t) \subset (\mathring{\mathbf{W}}_{k+1}^+)^{\circ} \xrightarrow{D_k^t} \mathcal{R}(\mathbb{T}_{k+1}^t) \subset (\mathring{\mathbf{W}}_{k+2}^+)^{\circ} \xrightarrow{D_{k+1}^t} \dots$$

is a Hilbert complex (the D_k^t s densely defined, closed on $(\mathring{\mathbf{W}}_{k+1}^+)^{\circ}$).

A simple criterion ensures that the trace Hilbert complex is Fredholm:

Theorem 6 (Fredholm property of trace Hilbert complex, [2, Thm. 7.3]). *If the inclusions $\mathbf{W}_k^+ \hookrightarrow \mathbf{W}_k$ are compact for all $k \in \mathbb{Z}$, then the embeddings*

$$\mathcal{D}(D_k^t) \cap \mathcal{D}((D_{k-1}^t)^*) \hookrightarrow (\mathring{\mathbf{W}}_{k+1}^+)^{\circ} \quad \text{are compact.}$$

REFERENCES

[1] D. N. ARNOLD AND K. HU, *Complexes from complexes*, Found. Comput. Math., 21 (2021), pp. 1739–1774.
 [2] R. HIPTMAIR, D. PAULY, AND E. SCHULZ, *Traces for Hilbert complexes*, Tech. Rep. 2022-07, Seminar for Applied Mathematics, ETH Zürich, Switzerland, 2022. arXiv:2203.00630 [math.FA].

Boundary Integral Exterior Calculus

ERICK SCHULZ

(joint work with Ralf Hiptmair and Stefan Kurz)

Applying the so-called tangential and normal traces $\mathbf{t} = \iota^*$ and $\mathbf{n} = \star^{-1} \iota^* \star$ to the de Rham complex in a Lipschitz subdomain Ω of a manifold \mathcal{M} , we obtain the trace de Rham complexes (see [6, 8] and the recent work “Traces for Hilbert complexes” [3])

$$(1a) \quad \dots \xrightarrow{d_{\ell-1}} H_{\perp}^{-\frac{1}{2}} \Lambda^{\ell-1}(d, \Gamma) \xrightarrow{d_{\ell}} H_{\perp}^{-\frac{1}{2}} \Lambda^{\ell}(d, \Gamma) \xrightarrow{d_{\ell+1}} \dots,$$

$$(1b) \quad \dots \xleftarrow{\delta_{\ell-1}} H_{\parallel}^{-\frac{1}{2}} \Lambda^{\ell-1}(\delta, \Gamma) \xleftarrow{\delta_{\ell}} H_{\parallel}^{-\frac{1}{2}} \Lambda^{\ell}(\delta, \Gamma) \xleftarrow{\delta_{\ell+1}} \dots,$$

on the boundary $\Gamma = \partial\Omega$, respectively. We equip these spaces with the non-local inner products [7, Thm. 3.6] (also see [1])

$$(2a) \quad \langle u, v \rangle_{-\frac{1}{2}, \lambda, \mathbf{t}} = \langle \mathbf{tS}^{\lambda}(u), \bar{v} \rangle_{\Gamma}, \quad u, v \in H_{\parallel}^{-\frac{1}{2}} \Lambda^{\ell}(\Gamma),$$

$$(2b) \quad \langle w, z \rangle_{-\frac{1}{2}, \lambda, \mathbf{n}} = \langle \mathbf{nD}(w), \bar{z} \rangle_{\Gamma}, \quad w, z \in H_{\perp}^{-\frac{1}{2}} \Lambda^{\ell}(\Gamma),$$

involving the boundary potentials [7, Eq. 3.8]

$$(3) \quad \mathbf{S}u(x) = \langle u, \mathbf{tG}(x, \cdot) \rangle_{\Gamma}, \quad \text{and} \quad \mathbf{D}w(x) = \langle w, \mathbf{nG}(x, \cdot) \rangle_{\Gamma},$$

where \mathcal{G} is a fundamental solution [7, Sec. 3] for the Hodge–Laplace or Yukawa operator (see [7, Sec. 3] and [2, 4, 5])

$$(4) \quad -\Delta + \lambda = d\delta + \delta d + \lambda.$$

The gist of Boundary Integral Exterior Calculus is the observation that two commutation identities are available which greatly simplify the derivation of boundary integral equations for operators related to the Hodge–Laplace/Yukawa operator acting on forms of order ℓ and to the (possibly perturbed) Hodge–Dirac operator

$$(5) \quad \mathfrak{D} + i\kappa = \mathbf{d} + \delta + i\kappa$$

acting on the full graded algebra of differential forms:

I. The pullback commutes with exterior differentiation as [7, Eq. 1.11]

$$(6) \quad \mathbf{t} \circ \mathbf{d} = \mathbf{d} \circ \mathbf{t} \quad \text{and} \quad \mathbf{n} \circ \delta = -\delta \circ \mathbf{n}.$$

II. The boundary potentials commute with exterior differentiation as [7, Lem. 3.1] (cf. [5, Lem. 3])

$$(7) \quad \delta \mathbf{S}(v) = \mathbf{S}(\delta v) \quad \text{and} \quad \mathbf{dD}(u) = -\mathbf{D}(du).$$

Since $\partial\Gamma = \emptyset$, integrating by parts then reveals that

$$(8a) \quad \langle \mathbf{tS}^{\lambda}(u), \bar{v} \rangle_{\Gamma} = \langle \delta^* u, v \rangle_{-\frac{1}{2}, \lambda, \mathbf{t}}, \quad \langle \mathbf{t}\delta \mathbf{S}^{\lambda}(u), \bar{v} \rangle_{\Gamma} = \langle \delta u, v \rangle_{-\frac{1}{2}, \lambda, \mathbf{t}},$$

$$(8b) \quad \langle \mathbf{nD}(w), \bar{z} \rangle_{\Gamma} = -\langle dw, z \rangle_{-\frac{1}{2}, \lambda, \mathbf{n}}, \quad \langle \mathbf{n}\delta \mathbf{D}(w), \bar{z} \rangle_{\Gamma} = -\langle d^* w, z \rangle_{-\frac{1}{2}, \lambda, \mathbf{n}},$$

where d^* and δ^* are Hilbert space adjoint to the exterior derivative and codifferential under the non-local inner products (2a) and (2b). These identities are

crucial, because they make it possible to recognize that *the first-kind boundary integral operators for Hodge–Dirac and Hodge–Laplace operators are Hodge–Dirac and Hodge–Laplace operators themselves in the trace de Rham complexes.*

For example, suppose that a full form $\mathbf{U} \in L^2\Lambda(\mathcal{M})$ is compactly supported and that there exists $\mathbf{F} \in L^2\Lambda(\mathcal{M})$ such that $\mathbf{F}|_\Omega = (\mathfrak{D} + i\kappa)\mathbf{U}|_\Omega$ and $\mathbf{F}|_{\Omega^+} = (\mathfrak{D} + i\kappa)\mathbf{U}|_{\Omega^+}$. Then, one has the representation formula

$$(9) \quad \mathbf{U} = (\mathfrak{D} - i\kappa) (\mathbf{N}\mathbf{F} - \mathbf{S}_\lambda \llbracket \mathbf{n}\mathbf{U} \rrbracket + \mathbf{D}_\lambda \llbracket \mathbf{t}\mathbf{U} \rrbracket),$$

where \mathbf{N} is the Newton operator given by the integral transformation involving \mathcal{G} and $\llbracket \bullet \rrbracket$ denotes the jump of a trace across Γ . Taking average traces $\{\bullet\}$ on both sides of (9) yields the boundary integral operators

$$(10a) \quad \mathbf{V}[\mathfrak{D}] := \{\mathbf{t}\} (\mathfrak{D} - i\kappa) \mathbf{S}, \quad \mathbf{K}[\mathfrak{D}] := \{\mathbf{t}\} (\mathfrak{D} - i\kappa) \mathbf{D},$$

$$(10b) \quad \mathbf{A}[\mathfrak{D}] := \{\mathbf{n}\} (\mathfrak{D} - i\kappa) \mathbf{S}, \quad \mathbf{W}[\mathfrak{D}] := \{\mathbf{n}\} (\mathfrak{D} - i\kappa) \mathbf{D},$$

that enter the variational formulations

$$(11a)$$

$$\mathbf{h} \in H_{\parallel}^{-\frac{1}{2}}\Lambda(\boldsymbol{\delta}, \Gamma) : \langle \mathbf{V}[\mathfrak{D}]\mathbf{h}, \overline{\mathbf{w}} \rangle_\Gamma = \langle (\frac{1}{2}\text{Id} + \mathbf{K}[\mathfrak{D}])\mathbf{g}, \overline{\mathbf{w}} \rangle_\Gamma, \quad \forall \mathbf{w} \in H_{\parallel}^{-\frac{1}{2}}\Lambda(\boldsymbol{\delta}, \Gamma),$$

$$(11b)$$

$$\mathbf{g} \in H_{\perp}^{-\frac{1}{2}}\Lambda(\mathbf{d}, \Gamma) : \langle \mathbf{W}[\mathfrak{D}]\mathbf{g}, \overline{\mathbf{v}} \rangle_\Gamma = \langle (\frac{1}{2}\text{Id} - \mathbf{A}[\mathfrak{D}])\mathbf{h}, \overline{\mathbf{v}} \rangle_\Gamma, \quad \forall \mathbf{v} \in H_{\perp}^{-\frac{1}{2}}\Lambda(\mathbf{d}, \Gamma),$$

associated with first-kind direct boundary integral equations. But from the jump relations

$$(12a) \quad \llbracket \mathbf{t} \rrbracket \mathbf{S} = 0, \quad \llbracket \mathbf{t}\mathbf{d} \rrbracket \mathbf{S} = 0, \quad \llbracket \mathbf{t}\boldsymbol{\delta} \rrbracket \mathbf{S} = 0,$$

$$(12b) \quad \llbracket \mathbf{n} \rrbracket \mathbf{S} = 0, \quad \llbracket \mathbf{n}\mathbf{d} \rrbracket \mathbf{S} = -\text{Id}, \quad \llbracket \mathbf{n}\boldsymbol{\delta} \rrbracket \mathbf{S} = 0,$$

$$(12c) \quad \llbracket \mathbf{t} \rrbracket \mathbf{D} = 0, \quad \llbracket \mathbf{t}\mathbf{d} \rrbracket \mathbf{D} = 0, \quad \llbracket \mathbf{t}\boldsymbol{\delta} \rrbracket \mathbf{D} = \text{Id},$$

$$(12d) \quad \llbracket \mathbf{n} \rrbracket \mathbf{D} = 0, \quad \llbracket \mathbf{n}\mathbf{d} \rrbracket \mathbf{D} = 0, \quad \llbracket \mathbf{n}\boldsymbol{\delta} \rrbracket \mathbf{D} = 0,$$

that were used to establish those equations, we also find that $\mathbf{V}[\mathfrak{D}] = \mathbf{t} (\mathfrak{D} - i\kappa) \mathbf{S}_\lambda$ and $\mathbf{W}[\mathfrak{D}] = \mathbf{n}(\mathfrak{D} - i\kappa)\mathbf{D}$. Based on the previous identities (I) and (II), we can evaluate [7, Sec. 4.1.2]

$$(13a) \quad \langle \mathbf{V}[\mathfrak{D}]\mathbf{h}, \overline{\mathbf{w}} \rangle_\Gamma = (\boldsymbol{\delta}\mathbf{h}, \mathbf{w})_{-\frac{1}{2}, \lambda, \mathbf{t}} + (\mathbf{h}, \boldsymbol{\delta}\mathbf{w})_{-\frac{1}{2}, \lambda, \mathbf{t}} - i\kappa(\mathbf{h}, \boldsymbol{\delta}\mathbf{w})_{-\frac{1}{2}, \lambda, \mathbf{t}},$$

$$(13b) \quad \langle \mathbf{W}[\mathfrak{D}]\mathbf{g}, \overline{\mathbf{v}} \rangle_\Gamma = -(\mathbf{d}\mathbf{g}, \mathbf{v})_{-\frac{1}{2}, \lambda, \mathbf{n}} - (\mathbf{g}, \mathbf{d}\mathbf{w})_{-\frac{1}{2}, \lambda, \mathbf{n}} - i\kappa(\mathbf{g}, \mathbf{v})_{-\frac{1}{2}, \lambda, \mathbf{n}},$$

from which we discover that

$$(14) \quad \boxed{\mathbf{V}[\mathfrak{D}] = \boldsymbol{\delta} + \boldsymbol{\delta}^* - i\kappa \quad \text{and} \quad \mathbf{W}[\mathfrak{D}] = -(\mathbf{d} + \mathbf{d}^*) - i\kappa}$$

on the boundary.

More involved calculations reveals that the first-kind boundary integral operators for the Hodge–Laplacian are also Hodge–Laplace operators on the boundary. This is true for both the strong and the mixed formulation

$$\mathfrak{M} = \begin{pmatrix} -\text{Id} & \boldsymbol{\delta} \\ \mathbf{d} & \boldsymbol{\delta}\mathbf{d} + \lambda \end{pmatrix},$$

obtained by introducing an auxiliary unknown $V = \delta U$. Indeed, these operators admit the representation formulas [7, Prop. 4.5 and 4.6]

$$U = NF - (d \quad \text{Id}) \begin{pmatrix} S[[nU]] \\ S[[ndU]] \end{pmatrix} + (\text{Id} \quad \delta) \begin{pmatrix} D[[t\delta U]] \\ D[[tU]] \end{pmatrix}$$

and

$$\begin{pmatrix} V \\ U \end{pmatrix} = \begin{pmatrix} -d\delta - \lambda\text{Id} & \delta \\ d & \text{Id} \end{pmatrix} \left(\begin{pmatrix} NH \\ NF \end{pmatrix} - \begin{pmatrix} 0 \\ D[[tV]] + \delta D[[tU]] \end{pmatrix} + \begin{pmatrix} S[[nU]] \\ S[[ndU]] \end{pmatrix} \right)$$

that eventually leads to the boundary integral operators [7, Sec. 4.2]

$$(15a) \quad \boxed{V[\Delta] = V[\mathfrak{M}] = \begin{pmatrix} -\delta^*\delta - \lambda\text{Id} & \delta \\ \delta^* & \text{Id} \end{pmatrix}}$$

$$(15b) \quad \boxed{W[\Delta] = W[\mathfrak{M}] = \begin{pmatrix} \text{Id} & -d^* \\ -d_{\ell-1} & -d^*d - \lambda\text{Id} \end{pmatrix}}$$

formulated in the trace de Rham complex equipped with non-local inner products.

REFERENCES

- [1] A. Buffa, M. Costabel, and C. Schwab. Boundary element methods for Maxwell’s equations on non-smooth domains. *Numer. Math.*, 92(4):679–710, 2002.
- [2] Xavier Claeys and Ralf Hiptmair. First-kind boundary integral equations for the Hodge-Helmholtz operator. *SIAM J. Math. Anal.*, 51(1):197–227, 2019.
- [3] Ralf Hiptmair, Dirk Pauly, and Erick Schulz. Traces for hilbert complexes. *arXiv preprint arXiv:2203.00630*, 2022.
- [4] Stefan Kurz and Bernhard Auchmann. Differential forms and boundary integral equations for Maxwell-type problems. In *Fast boundary element methods in engineering and industrial applications*, volume 63 of *Lect. Notes Appl. Comput. Mech.*, pages 1–62. Springer, Heidelberg, 2012.
- [5] Dorina Mitrea, Irina Mitrea, Marius Mitrea, and Michael Taylor. *The Hodge-Laplacian*, volume 64 of *De Gruyter Studies in Mathematics*. De Gruyter, Berlin, 2016. Boundary value problems on Riemannian manifolds.
- [6] Dorina Mitrea, Marius Mitrea, and Mei-Chi Shaw. Traces of differential forms on Lipschitz domains, the boundary de Rham complex, and Hodge decompositions. *Indiana Univ. Math. J.*, 57(5):2061–2095, 2008.
- [7] Erick Schulz, Ralf Hiptmair, and Stefan Kurz. Boundary integral exterior calculus. *manuscript in preparation*, 2022.
- [8] Norbert Weck. Traces of differential forms on Lipschitz boundaries. *Analysis (Munich)*, 24(2):147–169, 2004.

Hybridization and postprocessing in finite element exterior calculus

ARI STERN

(joint work with Gerard Awanou, Maurice Fabien, and Johnny Guzmán)

This talk presents the results of the paper [5], in which we develop hybridization and postprocessing techniques for the Hodge–Laplace problem on differential k -forms in \mathbb{R}^n , within the framework of finite element exterior calculus (FEEC) [3, 4, 1]. The hybridized FEEC methods use discontinuous spaces of differential forms, enforcing continuity and boundary conditions using Lagrange multipliers on the element boundaries. Their solutions are seen to agree with those of the original, non-hybrid FEEC methods, and the Lagrange multipliers correspond to weak tangential and normal traces. This hybrid formulation enables static condensation: since only the Lagrange multipliers are globally coupled, the remaining internal degrees of freedom can be eliminated using an efficient local procedure, and the resulting Schur complement system can be substantially smaller than the original one. We also present a generalization of Stenberg postprocessing [11], which for $0 < k < n$ is shown to give new improved estimates.

The special cases $k = 0$ and $k = n$ are shown to recover known results on hybridization and postprocessing for the scalar Poisson equation. In particular, the case $k = n$ corresponds to the hybridized Raviart–Thomas [2] and Brezzi–Douglas–Marini [6] methods, and the postprocessing procedure is precisely that of Stenberg [11]. The case $k = 0$ corresponds to the more recent hybridization of the continuous Galerkin method by Cockburn, Gopalakrishnan, and Wang [8].

The hybrid and postprocessing schemes in the remaining cases $0 < k < n$ are new and, to the best of our knowledge, have not appeared in the literature even for the vector Poisson equation when $n = 2$ or $n = 3$. In particular, the hybridization of Nédélec edge elements is different from that in [7]: here, the Lagrange multipliers are simply traces of standard elements, rather than living in a space of “jumps.” We expect these new methods to be especially useful in computational electromagnetics, where Nédélec elements are ubiquitous and the differential forms point of view has provided significant insight [10].

While we restrict our attention primarily to hybrid methods for conforming simplicial meshes, we remark that the framework developed here has the potential to be applied to other types of domain decomposition methods, including methods on cubical meshes, nonconforming meshes, mortar methods, etc. We also discuss briefly how the unified hybridization framework of Cockburn, Gopalakrishnan, and Lazarov [9], which includes nonconforming and hybridizable discontinuous Galerkin (HDG) methods, may also be generalized to the Hodge–Laplace problem for $0 < k < n$.

REFERENCES

- [1] Douglas N. Arnold, *Finite element exterior calculus*, CBMS-NSF Regional Conference Series in Applied Mathematics, vol. 93, Society for Industrial and Applied Mathematics (SIAM), Philadelphia, PA, 2018.

- [2] D. N. Arnold and F. Brezzi, *Mixed and nonconforming finite element methods: implementation, postprocessing and error estimates*, RAIRO Modél. Math. Anal. Numér. **19** (1985), no. 1, 7–32.
- [3] Douglas N. Arnold, Richard S. Falk, and Ragnar Winther, *Finite element exterior calculus, homological techniques, and applications*, Acta Numer. **15** (2006), 1–155.
- [4] ———, *Finite element exterior calculus: from Hodge theory to numerical stability*, Bull. Amer. Math. Soc. (N.S.) **47** (2010), no. 2, 281–354.
- [5] Gerard Awanou, Maurice Fabien, Johnny Guzmán, and Ari Stern, *Hybridization and post-processing in finite element exterior calculus*, Math. Comp., in press. Preprint available at arXiv:2008.00149 [math.NA].
- [6] Franco Brezzi, Jim Douglas, Jr., and L. D. Marini, *Two families of mixed finite elements for second order elliptic problems*, Numer. Math. **47** (1985), no. 2, 217–235.
- [7] Bernardo Cockburn and Jayadeep Gopalakrishnan, *Incompressible finite elements via hybridization. II. The Stokes system in three space dimensions*, SIAM J. Numer. Anal. **43** (2005), no. 4, 1651–1672.
- [8] Bernardo Cockburn, Jayadeep Gopalakrishnan, and Haiying Wang, *Locally conservative fluxes for the continuous Galerkin method*, SIAM J. Numer. Anal. **45** (2007), no. 4, 1742–1776.
- [9] Bernardo Cockburn, Jayadeep Gopalakrishnan, and Raytcho Lazarov, *Unified hybridization of discontinuous Galerkin, mixed, and continuous Galerkin methods for second order elliptic problems*, SIAM J. Numer. Anal. **47** (2009), no. 2, 1319–1365.
- [10] R. Hiptmair, *Finite elements in computational electromagnetism*, Acta Numer. **11** (2002), 237–339.
- [11] Rolf Stenberg, *Postprocessing schemes for some mixed finite elements*, RAIRO Modél. Math. Anal. Numér. **25** (1991), no. 1, 151–167.

The bubble transform and the de Rham complex

RAGNAR WINTHER

(joint work with Richard S. Falk)

The purpose of this talk is to discuss a generalization of the bubble transform to differential forms. The bubble transform was discussed for scalar valued functions, or zero forms, in [2]. It represents a new tool for the understanding of finite element spaces of arbitrary polynomial degree. The present talk contains a similar study for differential forms. From a simplicial mesh \mathcal{T} of the domain Ω , we build a map which decomposes piecewise smooth k forms into a sum of local bubbles supported on appropriate macroelements. The key properties of the decomposition are that it commutes with the exterior derivative and preserves the piecewise polynomial structure of the standard finite element spaces of k -forms. Furthermore, the transform is bounded in L^2 and also on the appropriate subspace consisting of k -forms with exterior derivatives in L^2 .

We let $\Lambda^k(\mathcal{T})$ denote the set of piecewise smooth k forms with respect to the mesh \mathcal{T} . In the setting of finite element exterior calculus, there are two fundamental families of piecewise polynomial subspaces of $\Lambda^k(\mathcal{T})$. These are the spaces $\mathcal{P}_r\Lambda^k(\mathcal{T})$ and $\mathcal{P}_r^-\Lambda^k(\mathcal{T})$, where $r \geq 1$. The spaces $\mathcal{P}_r\Lambda^k(\mathcal{T})$ consist of all piecewise polynomial k -forms of degree r , while the spaces $\mathcal{P}_r^-\Lambda^k(\mathcal{T})$ consist of piecewise polynomial k -forms which locally on each subsimplex contain $\mathcal{P}_{r-1}\Lambda^k$, but are contained in $\mathcal{P}_r\Lambda^k$. In the special case $r = 1$, the space $\mathcal{P}_1^-\Lambda^k(\mathcal{T})$ is exactly the

Whitney forms associated to the mesh \mathcal{T} . For both these families of finite element spaces, there exist sets of degrees of freedom associated to elements of $\Delta(\mathcal{T})$ which uniquely determine the elements of the space. More precisely, an element u is uniquely determined by functionals of the form

$$(1) \quad u \mapsto \int_f \operatorname{tr}_f u \wedge \eta, \quad \eta \in \mathcal{P}'(f, k, r), \quad f \in \Delta(\mathcal{T}), \dim f \geq k,$$

where the test space $\mathcal{P}'(f, k, r) \subset \Lambda^{\dim f - k}(f)$. We refer to [1, Chapter 4], for more details. The degrees of freedom of the form (1) correspond to a decomposition of the dual space into local subspaces, and lead to a local basis, referred to as the dual basis for the spaces $\mathcal{P}_r \Lambda^k(\mathcal{T})$ and $\mathcal{P}_r^- \Lambda^k(\mathcal{T})$. A further consequence is that the spaces themselves admit a decomposition of the form

$$(2) \quad V^k(\mathcal{T}) = \bigoplus_{\substack{f \in \Delta_m(\mathcal{T}) \\ m \geq k}} V_f^k, \quad V_f^k \subset \mathring{\Lambda}^k(\mathcal{T}_f),$$

where $V^k(\mathcal{T})$ is a space of the form $\mathcal{P}_r \Lambda^k(\mathcal{T})$ or $\mathcal{P}_r^- \Lambda^k(\mathcal{T})$, and V_f^k is a space of functions in $V^k(\mathcal{T})$ with all degrees of freedom taken to be zero except the ones associated to the simplex f . More precisely, a function $u \in V^k(\mathcal{T})$ admits a decomposition

$$u = \sum_{\substack{f \in \Delta_m(\mathcal{T}) \\ m \geq k}} u_f, \quad u_f \in V_f^k,$$

and the map $u \mapsto \{u_f\}$ is implicitly given by the degrees of

$$\operatorname{tr}_f \sum_{j=k}^m u_j = \operatorname{tr}_f u, \quad f \in \Delta_m(\mathcal{T}), k \leq m \leq n,$$

where $u_j = \sum_{g \in \Delta_j(\mathcal{T})} u_g$ and where tr denotes the trace operator. The map $u \mapsto \{u_f\}$ depends heavily on the particular space $V^k(\mathcal{T})$, and in particular on the polynomial degree r . On the other hand, the geometry of the decomposition (2), represented by the macroelements Ω_f and the associated mesh \mathcal{T}_f , is independent of the choice of discrete spaces. This indicates that it might be possible to define the map $u \mapsto \{u_f\}$ independent of the choice of discrete spaces. With some modifications, this is what we achieve by the construction presented in this talk.

REFERENCES

- [1] Douglas N. Arnold, Richard S. Falk, and Ragnar Winther, *Finite element exterior calculus, homological techniques, and applications*, Acta Numerica **15** (2006), 1–155.
- [2] Richard S. Falk and Ragnar Winther, *The Bubble Transform: A New Tool for Analysis of Finite Element Methods*, Found. Comput. Math., **16** (2016), no. 1, 297–328.

BGG sequences of tensor product finite elements with arbitrary continuity

FRANCESCA BONIZZONI

(joint work with Kaibo Hu, Guido Kanschat, Duygu Sap)

Starting from the well-understood de Rham complex, it is possible to derive new complexes and deduce their properties from those of the starting complex. This construction is related to the Bernstein-Gelfand-Gelfand (BGG) sequence, and its first systematic study is due to [2]. Recently, there has been a growing interest in discretizing special cases of BGG complexes. Nevertheless, a systematic construction of discrete BGG complexes is still missing.

In the present work (based on [3]) we provide a recipe to derive discrete BGG diagrams and BGG complexes of arbitrary dimension on Cartesian meshes. The construction is based on tensor product for complexes of differential forms introduced in [1], and its building block are the one-dimensional finite element (FE) cochain complexes of arbitrary continuity presented in [4, 5].

Let $\{\mathcal{S}_r\}_{r \geq 0}$ be the family of FE subspaces of polynomials of degree r on the reference interval $\mathcal{I} = [0, 1]$, and denote with $\mathcal{S}_{r-i}\Lambda^i := \mathcal{S}_{r-i} \otimes \text{Alt}^i$ the finite dimensional space of FE differential i -forms on $\mathcal{I} = [0, 1]$, for $i = 0, 1$. We assume that the following sequence is an exact complex:

$$(1) \quad 0 \longrightarrow \mathbb{R} \longrightarrow \mathcal{S}_r\Lambda^0 \xrightarrow{d} \mathcal{S}_{r-1}\Lambda^1 \longrightarrow 0.$$

Examples of exact FE complexes can be found in [4, 5]. Tensorizing the spaces in (1) with j -alternating forms Alt^j , for $j = 0, 1$, we obtain

$$(2) \quad \mathcal{S}_r\Lambda^{i,j} := \mathcal{S}_{r-i-j} \otimes \text{Alt}^i \otimes \text{Alt}^j,$$

namely, spaces of alternating i, j -forms with coefficients in \mathcal{S}_{r-i-j} . They form the following BGG diagram:

$$(3) \quad \begin{array}{ccccccc} 0 & \longrightarrow & \mathcal{S}_r\Lambda^{0,0} & \xrightarrow{d} & \mathcal{S}_{r-1}\Lambda^{1,0} & \longrightarrow & 0 \\ & & & \nearrow S^{0,1} & & & \\ 0 & \longrightarrow & \mathcal{S}_{r-1}\Lambda^{0,1} & \xrightarrow{d} & \mathcal{S}_{r-2}\Lambda^{1,1} & \longrightarrow & 0 \end{array}$$

Note, in particular, that the operator $S^{0,1}$ is bijective and, in a vector proxy with canonical bases, it boils down to the identity operator. The BGG construction yields the following complex:

$$(4) \quad 0 \longrightarrow \Upsilon^0 \xrightarrow{\mathcal{D}} \Upsilon^1 \longrightarrow 0$$

with spaces

$$\Upsilon^0 := \mathcal{S}_r\Lambda^{0,0}, \quad \Upsilon^1 := \mathcal{S}_{r-2}\Lambda^{1,1},$$

and the operator

$$\mathcal{D} = d(S^{0,1})^{-1}d.$$

Given a non-negative integer I , we define the set of characteristic multi-indices

$$X_I := \left\{ \mathbf{t} = (t_1, \dots, t_n) \in \{0, 1\}^n \left| \sum_{j=1}^n t_j = I \right. \right\}.$$

Let be given a multi-index $\mathbf{r} = (r_1, \dots, r_n)$, where r_i denotes the polynomial degree in the i^{th} direction. The tensor product construction yields to

$$\mathcal{S}_{\mathbf{r}}\Lambda^{I,J} := \bigoplus_{\substack{(i_1, \dots, i_n) \in X_I \\ (j_1, \dots, j_n) \in X_J}} (\mathcal{S}_{r_1-i_1-j_1} \otimes \dots \otimes \mathcal{S}_{r_n-i_n-j_n}) \otimes \text{Alt}^{i_1, j_1} \otimes \dots \otimes \text{Alt}^{i_n, j_n}.$$

The spaces $\{\mathcal{S}_{\mathbf{r}}\Lambda^{I,J}\}_{I,J}$ form the following tensor product BGG diagram

$$(5) \quad \begin{array}{ccccccc} \dots & \longrightarrow & \mathcal{S}_{\mathbf{r}}\Lambda^{I-1, J-1} & \xrightarrow{d} & \mathcal{S}_{\mathbf{r}}\Lambda^{I, J-1} & \xrightarrow{d} & \mathcal{S}_{\mathbf{r}}\Lambda^{I+1, J-1} & \longrightarrow & \dots \\ & & \nearrow & \xrightarrow{S^{I-1, J}} & \nearrow & \xrightarrow{S^{I, J}} & \nearrow & & \\ \dots & \longrightarrow & \mathcal{S}_{\mathbf{r}}\Lambda^{I-1, J} & \xrightarrow{d} & \mathcal{S}_{\mathbf{r}}\Lambda^{I, J} & \xrightarrow{d} & \mathcal{S}_{\mathbf{r}}\Lambda^{I+1, J} & \longrightarrow & \dots \end{array}$$

where $d: \mathcal{S}_{\mathbf{r}}\Lambda^{I,J} \rightarrow \mathcal{S}_{\mathbf{r}}\Lambda^{I+1,J}$ and $S^{I,J}: \mathcal{S}_{\mathbf{r}}\Lambda^{I,J} \rightarrow \mathcal{S}_{\mathbf{r}}\Lambda^{I+1, J-1}$. Following the BGG recipe, we then derive the following BGG complex:

$$(6) \quad 0 \longrightarrow \Upsilon^0 \xrightarrow{\mathcal{D}^0} \Upsilon^1 \xrightarrow{\mathcal{D}^1} \dots \xrightarrow{\mathcal{D}^{n-1}} \Upsilon^n \longrightarrow 0$$

with spaces

$$\Upsilon^K := \begin{cases} \mathcal{S}_{\mathbf{r}}\Lambda^{K, J-1} \cap \mathcal{R}(S^{K-1, J})^\perp, & K < J; \\ \mathcal{S}_{\mathbf{r}}\Lambda^{K, J} \cap \ker(S^{K, J}), & K \geq J, \end{cases}$$

and operators

$$\mathcal{D}^K := \begin{cases} P_{\mathcal{R}(S^{K-1, J})^\perp} d, & K \leq J - 1; \\ d \circ (S^{K-1, J})^{-1} \circ d, & K = J; \\ d, & K \geq J + 1. \end{cases}$$

Let us now assume that there exists $\pi^{i,j}: L^2\Lambda^{i,j}(\mathcal{I}) \rightarrow \mathcal{S}_{\mathbf{r}}\Lambda^{i,j}(\mathcal{I})$, for $i, j = 0, 1$, such that it is L^2 -stable and it commutes with the exterior derivative d as well as with $S^{i,j}$. Examples of such quasi-interpolation operators can be found in [4, 5]. Following the tensor product construction, we define

$$\pi_{\otimes n}^{I,J} := \bigoplus_{\substack{(i_1, \dots, i_n) \in X_I \\ (j_1, \dots, j_n) \in X_J}} (\pi^{i_1, j_1} \otimes \dots \otimes \pi^{i_n, j_n}).$$

The tensor product operator $\pi_{\otimes n}^{I,J}$ maps the space of I, J -forms on $\mathcal{I}^{\times n}$ with L^2 -regular coefficients to $\mathcal{S}_{\mathbf{r}}^p\Lambda^{I,J}$. It can be proved that $\pi_{\otimes n}^{I,J}$ is L^2 -stable and it commutes with the operators d and $S^{I,J}$ forming the tensor product BGG diagram (5). As a result, we have equipped the tensor product BGG complex (6) with commuting quasi-interpolation operators.

REFERENCES

- [1] D.N. Arnold, D. Boffi and F. Bonizzoni. *Finite element differential forms on curvilinear cubic meshes and their approximation properties*, Numerische Mathematik **129**: 1 (2015), 1 – 20.
- [2] D.N. Arnold, and K. Hu. *Complexes from complexes*, Foundations of Computational Mathematics **21**: 6 (2021), 1739–1774.
- [3] F. Bonizzoni, K. Hu, G. Kanschat and D. Sap. *Spline and tensor product finite element BGG sequences*, In preparation.
- [4] F. Bonizzoni and G. Kanschat. *H^1 -conforming finite element cochain complexes and commuting quasi-interpolation operators on cartesian meshes*, Calcolo **58**: 18 (2021).
- [5] F. Bonizzoni and G. Kanschat. *A tensor product finite element cochain complex with arbitrary continuity*. arXiv:2207.00309.

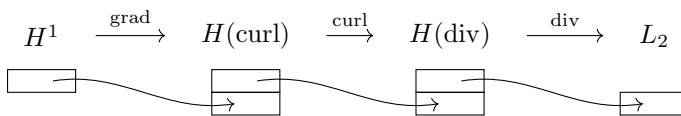
Matrix-valued Finite Elements with Applications in Elasticity and Curvature

JOACHIM SCHÖBERL

Vector-valued function spaces, their finite element sub-spaces, and relations between these spaces are well understood within the de Rham complex. The framework of differential forms and Hilbert complexes provides a unified framework for any space dimension.

Various matrix-valued finite element spaces have been introduced and analyzed more or less independently. In this report we put these spaces into a so called 2-complex. We consider function spaces on $\Omega \subset \mathbb{R}^3$.

The vector-valued spaces are $H(\text{curl}) = \{v \in L_2(\mathbb{V}) : \text{curl} u \in L_2(\mathbb{V})\}$ and $H(\text{div}) = \{v \in L_2(\mathbb{V}) : \text{div} u \in L_2\}$, with $\mathbb{V} := \mathbb{R}^3$. We consider the de Rham sequence



The boxes below the space represent direct sums of sub-spaces. E.g. $H(\text{curl})$ can be decomposed into the range of grad , and a sub-space on which the curl is regular. Similar for $H(\text{div})$, and also at the end of the sequence with trivial sub-spaces.

The differential operators commute with proper boundary traces, e.g. the tangential gradient of an H^1 function is the same as the tangential trace of its gradient in $H(\text{curl})$. The canonical traces are reflected in the continuity properties of finite elements, e.g. tangential-continuous Nédélec elements \mathcal{N}^k and normal-continuous Raviart-Thomas \mathcal{RT}^k or Brezzi-Douglas-Marini elements \mathcal{BDM}^k .

We introduce the matrix valued spaces

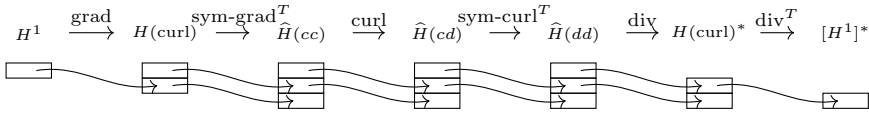
$$\begin{aligned}
 \widehat{H}(dd) & := \{\sigma \in H^{-1}(\mathbb{S}) : \text{div} \sigma \in H^{-1}(\mathbb{V}), \text{div} \text{div} \sigma \in H^{-1}(\mathbb{R})\}, \\
 \widehat{H}(cd) & := \{\sigma \in H^{-1}(\mathbb{T}) : \text{div} \sigma \in H^{-1}(\mathbb{V}), \text{sym-curl}^T \sigma \in H^{-1}(\mathbb{S}), \text{curl} \text{div} \sigma \in H^{-1}(\mathbb{V})\}, \\
 \widehat{H}(cc) & := \{\sigma \in H^{-1}(\mathbb{S}) : \text{curl} \sigma \in H^{-1}(\mathbb{T}), \text{curl}^T \text{curl} \sigma \in H^{-1}(\mathbb{S})\},
 \end{aligned}$$

with $\mathbb{S} = \{\sigma \in \mathbb{R}^{3 \times 3} : \sigma = \sigma^T\}$, $\mathbb{T} = \{\eta \in \mathbb{R}^{3 \times 3} : \text{tr } \eta = 0\}$. A differential operator is applied to a matrix row-wise, and \cdot^T means that it is applied column-wise. The prefix sym takes the symmetric part of the result.

This spaces are less regular than L_2 . To define L_2 -like energy norms, we need the regular sub-spaces

$$\begin{aligned} \tilde{H}(dd) &:= \{\sigma \in L_2(\mathbb{S}) : \text{div div } \sigma \in H^{-1}(\mathbb{R})\}, \\ \tilde{H}(cd) &:= \{\sigma \in L_2(\mathbb{T}) : \text{curl div } \sigma \in H^{-1}(\mathbb{V})\}, \\ \tilde{H}(cc) &:= \{\sigma \in L_2(\mathbb{S}) : \text{curl}^T \text{curl } \sigma \in H^{-1}(\mathbb{S})\}. \end{aligned}$$

Together with the scalar and vector-valued spaces we can put these spaces into a sequence:



Defining $A_0 = \text{grad}$, $A_1 = \text{sym-grad}^T$, and so on, we can easily verify that

$$A_{i+2}A_{i+1}A_i = 0,$$

i.e. three operators in a row vanish. This is called a **2-complex**. The boxes below the matrix-valued spaces represent sub-spaces. The box at the head of an arrow represents the range of the operator applied to the sub-space associated to the box at the arrow tail. E.g. the the space $\tilde{H}(cc)$ is decomposed into three sub-spaces: The bottom box is the range of the second order operator $\text{hess} := \text{sym-grad}^T \text{grad}$. This sub-space is exactly the null-space of the next, first order operator curl . The middle box is the range of the first order operator sym-grad^T , applied to the complement space of the gradient sub-space within $H(\text{curl})$. Restricted to the middle box the curl operator is regular, but the second order operator $\text{inc} := \text{sym-curl}^T \text{curl}$ vanishes. On the sub-space of the upper box the second order operator inc is regular. Understanding the cohomology spaces of this 2-complex is ongoing research.

By forming different combinations of two first order operators to a second order operator, we can recover the following complexes, which are exact:

- Elasticity complex

$$H(\text{curl}) \xrightarrow{\text{def}} H(cc) \xrightarrow{\text{inc}} H(dd) \xrightarrow{\text{div}} H(\text{curl})^*$$

- Hessian complex (using $\text{div sym-curl} = \frac{1}{2} \text{curl div}$):

$$H^1 \xrightarrow{\text{hess}} H(cc) \xrightarrow{\text{curl}} H(cd) \xrightarrow{\text{div}} H(\text{div})^* \xrightarrow{\text{div curl}^0} 0$$

- div div complex (using $\text{curl sym-grad} = \frac{1}{2} \text{dev grad curl}$):

$$0 \xrightarrow{\text{curl grad}^0} H(\text{curl}) \xrightarrow{\text{dev grad}} H(cd) \xrightarrow{\text{sym-curl}^T} H(dd) \xrightarrow{\text{div div}} H^{-1}$$

Finite element spaces for the matrix-valued function spaces are defined similarly as for vector-valued spaces, with certain continuity constraints for normal and

tangential components. Now, we multiply the matrix with normal or tangential vectors from the left and from the right:

$$\begin{aligned} V_{dd}^k &= \{ \sigma \in L_2(\mathbb{S}) : \sigma|_T \in P^k(\mathbb{S}), \sigma_{nn} \text{ continuous} \} \\ V_{cd}^k &= \{ \sigma \in L_2(\mathbb{T}) : \sigma|_T \in P^k(\mathbb{T}), \sigma_{nt} \text{ continuous} \} \\ V_{cc}^k &= \{ \sigma \in L_2(\mathbb{S}) : \sigma|_T \in P^k(\mathbb{S}), \sigma_{tt} \text{ continuous} \} \end{aligned}$$

These spaces are slightly non-conforming. In 2D, V_{dd}^k is the Hellan-Herrmann-Johnson finite element space, used for Kirchhoff plates [3]. It was extended to 3D for the TDNNS method for elasticity [13, 12]. The $H(\text{curl div})$ space and V_{cd} finite elements were introduced in [6, 4] for the MCS method for the Navier-Stokes equations. The V_{cc} is the Regge finite element space, which was brought by [2, 7] into the finite element framework with applications in relativity, see also [8, 5, 9].

All finite element spaces start from lowest order $k = 0$, and can be defined as usual by mapping from a reference element. This easily allows curved elements, and also elements mapped to manifolds.

To solve variational problems we have to verify well-posedness of operators. It is easy to show continuity

$$\forall u \in H(\text{curl}) \forall \sigma \in H(dd) : \quad \langle \text{div } \sigma, v \rangle \leq \| \sigma \|_{\widehat{H}(dd)} \| u \|_{H(\text{curl})}$$

as well as the stability condition

$$\forall u \in H(\text{curl}) \exists \sigma \in H(dd) : \quad \frac{\langle \text{div } \sigma, u \rangle}{\| \sigma \|_{H(dd)} \| u \|_{H(\text{curl})}} \geq \beta$$

for both versions, $\widehat{H}(dd)$ and $\widetilde{H}(dd)$.

Most of the derivatives within the sequence are not defined as weak derivatives, but must be understood in distributional sense. Consider $\sigma \in V_{dd}^k$, and evaluate its distributional divergence $f := \text{div } \sigma$:

$$\begin{aligned} \langle f, \varphi \rangle &= - \int \sigma : \nabla \varphi = - \sum_T \int_T \sigma : \nabla \varphi = \sum_T \int_T \text{div } \sigma - \int_{\partial T} \sigma_n \varphi \\ &= \sum_T \int_T \text{div } \sigma \varphi - \sum_E \int_E [\sigma_n] \varphi = \sum_T \int_T \underbrace{\text{div } \sigma}_f \varphi - \sum_E \int_E \underbrace{[\sigma_{nt}]}_{f_E} \varphi \end{aligned}$$

$f = \text{div } \sigma$ consists of element-terms $f_T = \text{div}_T \sigma$, and facet-terms $f_E = [\sigma_{nt}]$. Since the facet term acts in tangential direction, this distribution can be applied to Nédélec finite element functions \mathcal{N}^k , which have single valued tangential traces on facets. We write the duality pairing as

$$\langle \text{div } \sigma, v \rangle \quad \text{for } \sigma \in V_{dd}^k, v \in \mathcal{N}^k$$

We can continue with the second distributional divergence $\text{div div } \sigma$ and obtain a distribution which can be applied to H^1 -conforming finite elements \mathcal{L}^k . Due to the arising point measures (2D) or edge measures (3D), $\text{div div } \sigma \notin H^{-1}$, and thus the finite element space is non-conforming.

There are many more pairings which can be built by distributional operators applied to these finite element spaces, e.g. $\langle \text{hess } w, \sigma \rangle$, $\langle \text{def}(u), \sigma \rangle$, $\langle \text{curl def}(u), \eta^T \rangle$,

$\langle \text{curl } \gamma, \eta^T \rangle, \langle \text{inc } \gamma, \tilde{\gamma} \rangle, \langle \text{sym-curl } \eta, \gamma \rangle, \langle \text{div } \eta, q \rangle, \langle \text{div } \sigma, u \rangle, \langle \text{div div } \sigma, w \rangle$ with $w \in \mathcal{L}^k \subset H^1$, $u \in \mathcal{N}^k \subset H(\text{curl})$, $q \in \mathcal{BDM}^k \subset H(\text{div})$, $\gamma \in V_{cc}^k \subset \tilde{H}(cc)$, $\eta \in V_{cd}^k \subset \tilde{H}(cd)$, $\sigma \in V_{dd}^k \subset \tilde{H}(dd)$.

These distributional pairings allow the construction of many finite element methods having additional robustness properties, e.g.

TDNNS method for elasticity: find stress $\sigma \in V_{dd}^k$ and displacement $u \in \mathcal{N}^k$

$$\begin{aligned} \int A\sigma : \tau + \langle \text{div } \tau, u \rangle &= 0 \quad \forall \tau \in V_{dd} \\ \langle \text{div } \sigma, v \rangle &= f(v) \quad \forall v \in \mathcal{N} \end{aligned}$$

this method is robust for thin structures [13, 12].

MCS method for Stokes: Find $\sigma \in V_{cd}^k$, $u \in \mathcal{BDM}^k$, and $p \in P^{k-1}$:

$$\begin{aligned} \int A\sigma : \tau + \langle \text{div } \tau, u \rangle + \langle \text{div } u, q \rangle &= 0 \quad \forall \tau \in V_{cd}, \forall q \in P^{k-1} \\ \langle \text{div } \sigma, v \rangle + \langle \text{div } v, p \rangle &= f(v) \quad \forall v \in \mathcal{BDM}^k. \end{aligned}$$

It obtains an exactly divergence-free discrete velocity, and is pressure robust [6, 4].

The Hellan-Herrmann-Johnson (HHJ) method for Kirchhoff plates: Find bending moments $\sigma \in V_{dd}^k$ and vertical deflection $w \in \mathcal{L}^{k+1}$ [3]:

$$\begin{aligned} \int A\sigma : \tau + \langle \text{div } \tau, \nabla w \rangle &= 0 \quad \forall \tau \in V_{dd}^k \\ \langle \text{div } \sigma, \nabla v \rangle &= f(v) \quad \forall v \in \mathcal{L}^{k+1} \end{aligned}$$

TDNNS for Reissner Mindlin plates: Find $\sigma \in V_{dd}^k$ and $w \in \mathcal{L}^{k+1}$, $\beta \in \mathcal{N}^k$:

$$\begin{aligned} \int A\sigma : \tau + \langle \text{div } \tau, \beta \rangle &= 0 \quad \forall \tau \in V_{dd}^k \\ \langle \text{div } \sigma, \delta \rangle - \frac{1}{t^2} \langle \nabla w - \beta, \nabla v - \delta \rangle &= f(v) \quad \forall v \in \mathcal{L}^{k+1}, \forall \delta \in \mathcal{N}^k, \end{aligned}$$

It is free of locking for small t , and for $t \rightarrow 0$ the discrete RM solution converges to the solution of the HHJ method [11].

Computing curvature using V_{cc}^k finite elements is presented in the contribution by M. Neunteufel. We are faithful for many discussions at the MFO workshop on this topics, in particular with Kaibo Hu and Douglas Arnold.

REFERENCES

- [1] D. Braess, A.S. Pechstein, J. Schöberl, An equilibration-based a posteriori error bound for the biharmonic equation and two finite element methods, *IMA Journal of Numerical Analysis* 40 (2), 951–975, 2020
- [2] S.H. Christiansen, *On the linearization of Regge calculus*, *Numerische Mathematik* 119 (4) 613–640, 2011
- [3] M.I. Comodi, *The Hellan–Herrmann–Johnson method: Some new error estimates and postprocessing*, *Mathematics of Computation* 52 (185), 17–29, 1989
- [4] J. Gopalakrishnan, P.L. Lederer, J. Schöberl, *A mass conserving mixed stress formulation for the Stokes equations*, *IMA Journal of Numerical Analysis* 40 (3), 1838–1874, 2020
- [5] J. Gopalakrishnan, M. Neunteufel, J. Schöberl, M. Wardetzky, *Analysis of curvature approximations via covariant curl and incompatibility for Regge metrics*, arXiv:2206.09343
- [6] P.L. Lederer, *A Mass Conserving Mixed Stress Formulation for Incompressible Flows*, Dissertation, TU Wien, 2019
- [7] L. Li, *Regge Finite Elements with Applications in Solid Mechanics and Relativity*. PhD thesis, University of Minnesota, 2018.

- [8] M. Neunteufel, *Mixed Finite Element Methods for Nonlinear Continuum Mechanics and Shells*, Dissertation, TU Wien, 2021
- [9] M. Neunteufel, J. Schöberl, *Avoiding membrane locking with Regge interpolation*, Computer Methods in Applied Mechanics and Engineering 373, 113524, 2021
- [10] A.S. Pechstein, J. Schöberl, *An analysis of the TDNNS method using natural norms*, Numerische Mathematik 139 (1), 93-120, 2018
- [11] A.S. Pechstein, J. Schöberl, *The TDNNS method for Reissner-Mindlin plates*, Numerische mathematik 137 (3), 713-740, 2017
- [12] A.S. Pechstein, J. Schöberl, *Tangential-displacement and normal-normal-stress continuous mixed finite elements for elasticity*, M³AS 21 (08), 1761-1782, 2011
- [13] A.S. Sinwel (now Pechstein), *A New Family of Mixed Finite Elements for Elasticity*, Dissertation, JKU Linz, 2009

Analysis of curvature approximations via covariant curl and incompatibility for Regge metrics

MICHAEL NEUNTEUFEL

(joint work with Jay Gopalakrishnan, Joachim Schöberl, Max Wardetzky)

We consider d -dimensional Riemannian manifolds (M, \mathbf{g}) with metric tensor \mathbf{g} . The intrinsic curvatures are given in terms of the fourth order Riemannian curvature tensor \mathcal{R} . Regge calculus has originally been developed for solving Einstein field equations in a coordinate free manner [1]. The manifold M gets approximated by a symplectic net and the squared lengths at the edges are prescribed. This approach leads to a discretized tangential-tangential continuous metric tensor \mathbf{g}_h of \mathbf{g} . In terms of the angle deficit an approximated curvature is computed by summing the internal angles around $d - 2$ -dimensional sub-simplexes and the deviation from 2π indicates curvature. We present and discuss the high-order curvature approximation for two- and three-dimensional Riemannian manifolds and their convergence, where $M \subset \mathbb{R}^d$ and a triangulation \mathcal{T} of M is given.

Two-dimensional Riemannian manifolds. For Riemannian manifolds (M, \mathbf{g}) , $M \subset \mathbb{R}^2$, the Gauss curvature $K = \frac{1}{\det \mathbf{g}} \mathcal{R}_{1221}$ is the intrinsic curvature quantity. The lifted distributional Gauss curvature $K_h \in V_h^{k+1}$ of an approximated metric tensor $\mathbf{g}_h = \mathcal{I}_h^{\text{Reg},k} \mathbf{g} \in \text{Regge}_h^k$ is defined by solving for all $u_h \in V_h^{k+1}$ [4, 2]

$$\int_M K_h u_h \sqrt{\det \mathbf{g}_h} da = \sum_{T \in \mathcal{T}} \int_T K(\mathbf{g}_h) \sqrt{\det \mathbf{g}_h} u_h da + \sum_{E \in \mathcal{E}} \int_E \llbracket \kappa_g(\mathbf{g}_h) \rrbracket \sqrt{\mathbf{g}_{h,tt}} u_h dl + \sum_{V \in \mathcal{V}} \left(2\pi - \sum_{T \in \mathcal{T}: V \subset T} \angle_V^T(\mathbf{g}_h) \right) u_h(V).$$

Here, motivated by the Gauss–Bonnet theorem, $K(\mathbf{g}_h)$ denotes the element-wise Gauss curvature, $\llbracket \kappa_g(\mathbf{g}_h) \rrbracket$ the jump of geodesic curvature of \mathbf{g}_h at the edges, and the last term involves the angle deficit, where $\angle_V^T(\mathbf{g}_h)$ is the internal angle of T at the vertex V with respect to \mathbf{g}_h . Further,

$$\text{Regge}_h^k := \{ \boldsymbol{\sigma}_h \in \mathcal{P}^k(\mathcal{T}, \mathbb{R}_{\text{sym}}^{d \times d}) \mid \llbracket \boldsymbol{\sigma}_{h,tt} \rrbracket = 0 \text{ for all faces} \}$$

denotes the *tangential-tangential continuous Regge finite elements* of polynomial order k , $\mathcal{I}_h^{\text{Reg},k}$ the corresponding canonical interpolant [5], and V_h^k the Lagrangian finite element space. The tangential vector at an element boundary is given by t .

Linearizing the right-hand side of the distributional Gauss curvature leads to an integral representation, where the distributional version of the covariant incompatibility operator $\text{inc}_g = \text{curl}_g \text{curl}_g$ is involved. Exploiting the properties of the Regge interpolant we prove for $g_h = \mathcal{I}_h^{\text{Reg},k} g$ the convergence rate [2]

$$\|K(g) - K_h\|_{H^{-1}} \leq Ch^{k+1} (\|g\|_{W^{k+1,\infty}} + \|K(g)\|_{H^k}).$$

Using approximations $g_h \in \text{Regge}_h^k$ of g other than the canonical Regge interpolant convergence of one order less has been proven in [4, 3].

Three-dimensional Riemannian manifolds. For Riemannian manifolds $M \subset \mathbb{R}^3$ we consider the curvature operator $Q : M \rightarrow \mathbb{R}_{\text{sym}}^{3 \times 3}$ encoding the intrinsic curvatures. It is given in coordinates by the Riemannian curvature tensor with Einstein’s summation convention $Q^{ij} = -\frac{1}{4 \det g} \varepsilon^{ikl} \varepsilon^{jmn} \mathcal{R}_{klmn}$, where ε^{ijk} denotes the Levi-Civita symbol. To define the lifted distributional curvature operator $Q_h \in \text{Regge}_h^k$ in analogy to the 2D setting we cannot rely on the Gauss-Bonnet theorem, not being available in 3D. We propose in coordinate expression to solve for all $P_h \in \text{Regge}_h^k$

$$\begin{aligned} \int_M Q_h : P_h \sqrt{\det g_h} dx &= \sum_{T \in \mathcal{T}} \left(\int_T Q(g_h) : P_h \sqrt{\det g_h} dx \right. \\ &+ \left. \int_{\partial T} \frac{\sqrt{\det g_h}}{\text{cof}(g_h)_{nn}} n \otimes n \times \Gamma_{\bullet\bullet}^n : P_h da \right) + \sum_{E \in \mathcal{E}} \left(2\pi - \sum_{T \in \mathcal{T}: E \subset T} \angle_E^T(g_h) \right) P_{h,t_E t_E} dl. \end{aligned}$$

Here, $:$ and \otimes denote the Frobenius inner and dyadic outer product, respectively, $\text{cof}(\cdot)$ the cofactor matrix, and $(A \times B)^{ij} = \varepsilon^{ikl} \varepsilon^{jmn} A_{km} B_{ln}$ the tensor cross product of two matrices. Further, n and t_E are the face outer normal and edge tangential vectors, respectively, and ∂T denotes the element boundary of T . The face terms, which involve the Christoffel symbols of second kind Γ_{ij}^k , were derived by mollification and has strong similarities to the geodesic curvature in 2D, $\kappa_g(g_h) \sqrt{g_{h,tt}} = \frac{\sqrt{\det g_h}}{g_{h,tt}} \Gamma_{tt}^n = \frac{\sqrt{\det g_h}}{g_{h,tt}} \Gamma_{ij}^k t^i t^j n_k$.

REFERENCES

[1] Regge, T.: General relativity without coordinates. *Il Nuovo Cimento* (1955-1965) 19, 3 (1961), 558–571.
 [2] J. Gopalakrishnan, M. Neunteufel, J. Schöberl, M. Wardetzky, *Analysis of curvature approximations via covariant curl and incompatibility for Regge metrics*, arxiv.org/abs/2206.09343 (2022).
 [3] Y. Berchenko-Kogan, E. Gawlik, *Finite element approximation of the Levi-Civita connection and its curvature in two dimensions*, arxiv.org/abs/2111.02512 (2021).
 [4] E. Gawlik, *High-order approximation of Gaussian curvature with Regge finite elements*, *SIAM Journal on Numerical Analysis* 58(3), (2020), 1801–1821.
 [5] L. Li, *Regge Finite Elements with Applications in Solid Mechanics and Relativity*, PhD thesis, University of Minnesota, (2018).

Duality and symmetry in finite element exterior calculus

YAKOV BERCHENKO-KOGAN

In 2006, Arnold, Falk, and Winther developed finite element exterior calculus, generalizing the Lagrange, Raviart-Thomas, Brezzi-Douglas-Marini, and Nédélec elements using the language of differential forms. In their work, determining the degrees of freedom of these spaces relied on a Hodge-star-like duality between k -forms with vanishing trace and $(n - k)$ -forms of lower polynomial degree with no boundary conditions. However, the exact relationship between this duality map and the Hodge star remained a mystery. We show that, after a coordinate transformation $\lambda_i = u_i^2$ between the standard simplex and the standard sphere, the relationship becomes clear: On the sphere, the duality map is just the Hodge star times a bubble function.

More recently, there has also been interest in whether these finite element spaces have bases that are invariant with respect to the symmetries of the simplex, both for theoretical reasons and for practical reasons of exploiting symmetry to accelerate computation. For instance, the standard basis for Whitney k -forms associates a basis element to each k -face of the simplex, and hence symmetries of the simplex send basis elements to basis elements (up to sign). However, in general, symmetric bases for finite element exterior calculus spaces might not exist. Recently, Licht conjectured for which spaces and which polynomial degrees such bases exist; building on Licht's work, we resolve this conjecture.

In my talk, I outlined these results and the main elements of the proofs. For the symmetry results, the main technique was understanding the representation theory of the space $\mathcal{P}_r \Lambda^k(T^n)$ and $\mathcal{P}_r^- \Lambda^k(T^n)$ on which the symmetric group S_{n+1} acts by permuting the vertices of the standard simplex T^n , or, equivalently, permuting the barycentric coordinates. Every representation has a unique decomposition as a direct sum of irreducible representations, so we can answer the question of whether invariant bases exists in two steps:

- (1) determine the decomposition into irreducibles for $\mathcal{P}_r \Lambda^k(T^n)$ and $\mathcal{P}_r^- \Lambda^k(T^n)$, and
- (2) determine which direct sums of irreducibles have invariant bases and which do not.

It turns out that in two or three dimensions, these steps can be simplified slightly; it suffices to consider just the subgroup that cyclically permutes three vertices rather than the entire permutation group.

Meanwhile, for the duality results, the main steps of the proof are:

- (1) identify the spaces of differential forms on the sphere that one obtains after applying the coordinate transformation $\lambda_i = u_i^2$ to the spaces $\mathcal{P}_r \Lambda^k(T^n)$, $\mathcal{P}_r^- \Lambda^k(T^n)$, and the corresponding spaces with vanishing trace, and
- (2) show that applying the Hodge star on the sphere followed by multiplication by a bubble function yields isomorphisms between the appropriate spaces of differential forms on the sphere.

In the talk, I went through each of these items, highlighting the main ideas for each finite element space.

Discrete Elasticity Complex on Alfeld Splits

JAY GOPALAKRISHNAN

(joint work with Snorre Christiansen, Johnny Guzmán, Kaibo Hu)

We report on our construction [2] of a discrete elasticity complex of finite element spaces, complete with unisolvent degrees of freedom and cochain projections.

For smooth fields on a contractible domain $\Omega \subset \mathbb{R}^3$, the exactness of the Kröner complex, $\mathcal{R} \xrightarrow{\mathcal{C}} C^\infty \otimes \mathbb{V} \xrightarrow{\varepsilon} C^\infty \otimes \mathbb{S} \xrightarrow{\text{inc}} C^\infty \otimes \mathbb{S} \xrightarrow{\text{div}} C^\infty \otimes \mathbb{V} \rightarrow 0$, is classical. Here, \mathcal{R} denotes the space of rigid displacements, $\mathbb{V} = \mathbb{R}^3$, $\mathbb{S} = \text{sym}(\mathbb{R}^{3 \times 3})$ where $\text{sym}(M) = (M + M')/2$ for $M \in \mathbb{R}^{3 \times 3}$, $\varepsilon(v) = \text{sym}(\text{grad } v)$ for vector fields $v : \Omega \rightarrow \mathbb{V}$, $\text{inc } g = \text{curl}(\text{curl } g)'$ for matrix fields $g : \Omega \rightarrow \mathbb{S}$, and $\text{div } \sigma$ denotes the row-wise divergence of a matrix field $\sigma : \Omega \rightarrow \mathbb{S}$. Our discrete elasticity complex is obtained by mimicking a construction that gives a Sobolev space analogue of this smooth complex.

This construction, which we now describe, is based on the Bernstein-Gelfand-Gelfand (BGG) resolution [1]. Let $\text{skw}(M) = (M - M')/2$, $\mathbb{K} = \text{skw}(\mathbb{R}^{3 \times 3})$, $\text{mskw} : \mathbb{V} \rightarrow \mathbb{K}$ denote the operator with the property that $\text{mskw}(v)w = v \times w$ for vectors $v, w \in \mathbb{V}$, and $\text{vskw} = \text{mskw}^{-1} \circ \text{skw}$. Starting with the Stokes complex containing the Sobolev space $H^1(\text{curl}) = \{v \in H^1 \otimes \mathbb{V} : \text{curl } v \in H^1 \otimes \mathbb{V}\}$, we line up another smooth de Rham complex (whose exactness follows from [3]) to get

$$(1) \quad \begin{array}{ccccccc} H^2 \otimes \mathbb{V} & \xrightarrow{\text{grad}} & H^1(\text{curl}) \otimes \mathbb{V} & \xrightarrow{\text{curl}} & H^1 \otimes \mathbb{M} & \xrightarrow{\text{div}} & L^2 \otimes \mathbb{V} \\ & \nearrow \text{-mskw} & & \nearrow \mathbb{S} & & \nearrow 2\text{vskw} & \\ H^2 \otimes \mathbb{V} & \xrightarrow{\text{grad}} & H^1 \otimes \mathbb{M} & \xrightarrow{\text{curl}} & H(\text{div}) \otimes \mathbb{V} & \xrightarrow{\text{div}} & L^2 \otimes \mathbb{V} \end{array}$$

where $S\sigma = \sigma' - \text{tr}(\sigma)\delta$ is a bijection. It is easy to verify that the above diagram commutes. Hence, by the simple result of [2, Proposition 2.3] inspired by the BGG technique, we obtain the derived exact complex

$$(2) \quad \begin{bmatrix} H^2 \otimes \mathbb{V} \\ H^2 \otimes \mathbb{V} \end{bmatrix} \xrightarrow{[\text{grad}, \text{-mskw}]} H^1(\text{curl}) \otimes \mathbb{V} \xrightarrow{\text{curl}S^{-1}\text{curl}} H(\text{div}) \otimes \mathbb{V} \xrightarrow{\begin{bmatrix} 2\text{vskw} \\ \text{div} \end{bmatrix}} \begin{bmatrix} L^2 \otimes \mathbb{V} \\ L^2 \otimes \mathbb{V} \end{bmatrix} .$$

Noting that for symmetric matrix fields g , the middle operator's action reduces to $\text{inc } g$, we reconsider the above sequence after symmetrizing the contributions from the operator $[\text{grad}, \text{-mskw}]$, and replacing $H(\text{div}) \otimes \mathbb{V}$ by the kernel of vskw , denoted by $H(\text{div}, \mathbb{S})$. Then, the exactness of (2) implies the exactness of

$$(3) \quad H^2 \otimes \mathbb{V} \xrightarrow{\text{sym grad}} \text{sym}(H^1(\text{curl}) \otimes \mathbb{V}) \xrightarrow{\text{inc}} H(\text{div}, \mathbb{S}) \xrightarrow{\text{div}} L^2 \otimes \mathbb{V} .$$

The final step is to prove that the second space in (3) is the same as $H(\text{inc}) = \{g \in H^1 \otimes \mathbb{S} : \text{inc } g \in L^2 \otimes \mathbb{S}\}$, i.e., to prove that

$$(4) \quad \text{sym} (H^1(\text{curl}) \otimes \mathbb{V}) = H(\text{inc}).$$

To do so, for the \subseteq -direction, let $G \in H^1(\text{curl}) \otimes \mathbb{V}$. Then obviously $g = \text{sym } G$ is in $H^1 \otimes \mathbb{S}$. Moreover, since trace of $\text{curl sym } G$ vanishes, $\text{inc } g = \text{curl } S^{-1} \text{curl } G \in L^2 \otimes \mathbb{S}$. For the reverse \supseteq -direction, let $g \in H(\text{inc})$ and put $\sigma = \text{inc } g \in L^2 \otimes \mathbb{S}$. Then $\left[\begin{smallmatrix} 2\text{vskw} \\ \text{div} \end{smallmatrix} \right] \sigma = 0$ implies, by the exactness of (2), the existence of $z \in H^1(\text{curl}) \otimes \mathbb{V}$ such that $\sigma = \text{curl } S^{-1} \text{curl } z$. Hence $\text{curl } S^{-1} \text{curl}(g - z) = 0$, which implies the existence of a $v \in H^1 \otimes \mathbb{V}$ such that $S^{-1} \text{curl}(g - z) = \text{grad } v$. Since $\text{curl mskw} = S \text{grad}$, setting $G = g + \text{mskw}v$, we find that $\text{curl } G = \text{curl } g - S \text{grad } v = \text{curl } z \in H^1 \otimes \mathbb{V}$. Thus $g = \text{sym } G$ for a $G \in H^1(\text{curl})$, completing the proof of (4). Combining (4) and (3), we complete our derivation of the exact complex

$$(5) \quad \mathcal{R} \xrightarrow{\subseteq} H^2 \otimes \mathbb{V} \xrightarrow{\varepsilon} H(\text{inc}) \xrightarrow{\text{inc}} H(\text{div}, \mathbb{S}) \xrightarrow{\text{div}} L^2 \otimes \mathbb{V} \longrightarrow 0$$

using the BGG technique.

These arguments set the stage for our discrete analysis in [2], which, even if more complicated, can be viewed as resulting from a search for finite element analogues of the above-described simple ideas. We start by considering the standard de Rham complex of finite element spaces on an Alfeld split of a single tetrahedron, namely let W_r^k denote the usual polynomial $P_r \wedge^k$ spaces. Let L_r^k denote the product of $\binom{3}{k}$ copies of the degree r Lagrange space and let $S_r^k = \{w \in L_r^k : dw \in L_{r-1}^{k+1}\}$. Then, on a single (split) tetrahedron,

$$\begin{aligned} Z_r^0 &= S_r^0 && \subseteq H^2 \otimes \mathbb{V} \\ Z_r^1 &= \{\omega \in S_r^1 : \text{curl } \omega \text{ is } C^1 \text{ at vertices of } T\} && \subseteq H^1(\text{curl}) \otimes \mathbb{V} \\ Z_r^2 &= \{\omega \in L_r^2 : \omega \text{ is } C^1 \text{ at vertices of } T\} && \subseteq H^1 \otimes \mathbb{M} \\ Z_r^3 &= \{\omega \in W_r^3 : \omega \text{ is } C^0 \text{ at vertices of } T\} && \subseteq L^2 \otimes \mathbb{V} \end{aligned}$$

are subspaces of the spaces in the top row of (1) while

$$\begin{aligned} V_r^0 &= S_r^0 && \subseteq H^2 \otimes \mathbb{V} \\ V_r^1 &= \{\omega \in L_r^1 : \omega \text{ is } C^1 \text{ at vertices of } T\} && \subseteq H^1 \otimes \mathbb{M} \\ V_r^2 &= \{\omega \in W_r^2 : \omega \text{ is } C^0 \text{ at vertices of } T\} && \subseteq H(\text{div}) \otimes \mathbb{V} \\ V_r^3 &= W_r^3 && \subseteq L^2 \otimes \mathbb{V} \end{aligned}$$

are subspaces of the spaces in the bottom row of (1). For these subspaces, we are able to carry over the BGG construction (1). In particular, the diagram

$$\begin{array}{ccccccc} Z_{r+1}^0 \otimes \mathbb{V} & \xrightarrow{\text{grad}} & Z_r^1 \otimes \mathbb{V} & \xrightarrow{\text{curl}} & Z_{r-1}^2 \otimes \mathbb{V} & \xrightarrow{\text{div}} & Z_{r-2}^3 \otimes \mathbb{V} \\ & \nearrow -\text{mskw} & & \nearrow S & & \nearrow 2\text{vskw} & \\ V_r^0 \otimes \mathbb{V} & \xrightarrow{\text{grad}} & V_{r-1}^1 \otimes \mathbb{V} & \xrightarrow{\text{curl}} & V_{r-2}^2 \otimes \mathbb{V} & \xrightarrow{\text{div}} & V_{r-3}^3 \otimes \mathbb{V} \end{array}$$

commutes and, as proved in [2], its top and bottom rows are exact sequences for $r \geq 4$. Just as (2) is the derived from (1), this then implies the exactness of the derived complex

$$\begin{bmatrix} Z_{r+1}^0 \otimes \mathbb{V} \\ V_r^0 \otimes \mathbb{V} \end{bmatrix} \xrightarrow{[\text{grad}, -\text{mskw}]} Z_r^1 \otimes \mathbb{V} \xrightarrow{\text{curl} S^{-1} \text{curl}} V_{r-2}^2 \otimes \mathbb{V} \xrightarrow{[\text{2vskw}, \text{div}]} \begin{bmatrix} Z_{r-2}^3 \otimes \mathbb{V} \\ V_{r-3}^3 \otimes \mathbb{V} \end{bmatrix},$$

which is useful to understand mixed methods for elasticity with weakly imposed stress symmetry constructed using the last two spaces above.

Next, let $U_r^1 = \text{sym}(Z_r^1 \otimes \mathbb{V})$ and denote the kernel of vskw by $U_{r-2}^2 = \{\omega \in V_{r-2}^2 \otimes \mathbb{V} : \text{skw}\omega = 0\}$. Then, as before, we obtain a discrete analogue of (3):

$$Z_{r+1}^0 \otimes \mathbb{V} \xrightarrow{\varepsilon} U_r^1 \xrightarrow{\text{inc}} U_{r-2}^2 \xrightarrow{\text{div}} V_{r-3}^3 \otimes \mathbb{V}.$$

Finally to see that $U_r^1 = \text{sym}(Z_r^1 \otimes \mathbb{V})$ is an $H(\text{inc})$ -conforming subspace, we perform a discrete analogue of the argument that we used above to prove (4). This is detailed in [2, Theorem 5.6]. Renaming $Z_{r+1}^0 \otimes \mathbb{V}$ to U_{r+1}^0 and $V_{r-3}^3 \otimes \mathbb{V}$ to U_{r-3}^3 and handling the end cases, we thus obtain the discrete elasticity complex

$$\mathcal{R} \xrightarrow{\subset} U_{r+1}^0 \xrightarrow{\varepsilon} U_r^1 \xrightarrow{\text{inc}} U_{r-2}^2 \xrightarrow{\text{div}} U_{r-3}^3 \longrightarrow 0$$

for $r \geq 4$, a subcomplex of (5) on a single split tetrahedron.

It does not appear to be trivial to conclude that the local finite element elasticity complex on a single tetrahedron immediately yields the associated global finite spaces on a mesh of tetrahedra (due to the tricky supersmoothness properties of Alfeld splits). Therefore, global finite element spaces are developed in [2] using the laborious approach of repeating the BGG construction with the global analogues of each of the above local spaces (and proving exactness of the global finite element sequences as needed). Unisolvent degrees of freedom for the spaces in the discrete elasticity complex and characterizations of the inter-element continuity constraints of the global spaces can all be found among the further results proved in [2].

REFERENCES

- [1] A. ČAP, J. SLOVÁK, AND V. SOUČEK, *Bernstein-Gelfand-Gelfand sequences*, Annals of Mathematics, 154 (2001), pp. 97–113.
- [2] S. CHRISTIANSEN, J. GOPALAKRISHNAN, J. GUZMÁN, AND K. HU, *A discrete elasticity complex on three-dimensional Alfeld splits*, Preprint arXiv:2009.07744 (2020).
- [3] M. COSTABEL AND A. MCINTOSH, *On Bogovskiĭ and regularized Poincaré integral operators for de Rham complexes on Lipschitz domains*, Mathematische Zeitschrift, 265 (2010), pp. 297–320.

The *hp3D* Code with Applications to Modeling of Optical Amplifiers

LESZEK DEMKOWICZ, STEFAN HENNEKING

(joint work with Jacob Badger, Markus Melenk)

In the discretization of partial differential equations (PDEs) in weak form, the natural energy setting for functions often falls within the energy spaces forming the exact sequence,

$$H^1(\Omega) \xrightarrow{\nabla} H(\text{curl}, \Omega) \xrightarrow{\nabla \times} H(\text{div}, \Omega) \xrightarrow{\nabla \cdot} L^2(\Omega),$$

where $\Omega \subset \mathbb{R}^3$ denotes the domain in which the problem is being solved. This work presents advances in the implementation of the *hp3D* finite element (FE) software, which supports *conforming discretization* of the exact-sequence energy spaces. More precisely, *hp3D* supports the construction of *orientation-embedded shape functions* corresponding to Nédélec’s sequence of the first type [7] for elements of “all shapes:” tetrahedra, hexahedra, prisms, and pyramids. The *hp3D* code is documented in [2, 3, 15], and more recently in [11, 19, 14]. As of July 2022, a preliminary version of *hp3D*, and accompanying user manual [13], has been made available as open-source code at <https://github.com/Oden-EAG/hp3d>.

hp3D supports discretization of any system of PDEs involving unknowns from the exact-sequence spaces and possibly defined only on specific subdomains of Ω . It also supports the solution of weakly-coupled problems where one solves sequentially two or more different problems with unknowns defined on a common domain. As an example of a complex multiphysics application realized in *hp3D*, we present results for a Maxwell model of an optical fiber amplifier accompanied by stability analysis of a related linear waveguide problem.

The DPG method. Over the past decade, the *hp3D* code has served as a main research tool for the discontinuous Petrov–Galerkin (DPG) method. The DPG method offers an unprecedented *guaranteed* stability with no preasymptotic behavior. The stability comes from using *optimal test functions* that are computed *locally* on the fly. The local determination of optimal test functions is possible only because of the use of discontinuous test spaces [4]. The method can be classified as a *minimum residual method* with the residual measured in an (approximate) dual norm; it always delivers a positive definite Hermitian matrix, and it comes with a built-in a-posteriori error estimate [5]. DPG is a hybrid method with a group variable consisting of the solution defined on elements and additional *traces* that live on the mesh skeleton. The additional unknowns (traces) are discretized by using traces of standard element shape functions to the mesh skeleton [8, 6].

Advances in *hp3D*. Recent development of *hp3D* has been focused on the implementation of an adaptive DPG multilevel solver for wave propagation problems [17, 18, 19] and the hybrid parallelization of the code with MPI+OpenMP [11, 12]. These advancements are built on the code’s lean data structures, supporting *anisotropic refinements* in both element size h and polynomial order p . Such refinements are essential to obtaining optimal convergence in many problems (e.g., to resolve boundary layers). The parallel code has been designed to run

efficiently on small machines (e.g., a single workstation or laptop), as well as large-scale computing facilities (e.g., *Frontera* at the Texas Advanced Computing Center (TACC)). The mesh partitioning follows a hybrid MPI/OpenMP parallelization approach where mesh data is distributed to MPI processes and each MPI process uses OpenMP threading to parallelize its computational workload.

Optical amplifier. *hp3D* implements a vectorial Maxwell model of an ytterbium (Yb)-doped active gain fiber amplifier. The model is described in [10], and large-scale simulations for 10k wavelengths are shown in [9, 12]. In a nutshell, the model solves a nonlinear Maxwell problem describing the electromagnetic field inside the optical amplifier, weakly coupled to the transient heat equation. Both problems are discretized with the DPG method. At high power levels, the amplifier experiences a thermally-induced *transverse mode instability* (TMI) which must be suppressed to preserve the output beam quality.

Once we learned that the TMI-related fluctuations happen at the level of the modal interference pattern (thousands of wavelengths), the idea of using the so-called *full envelope ansatz* emerged. This ansatz for the (linear) Maxwell problem trades the original operator A for a new operator \tilde{A} defined as:

$$\tilde{A}\tilde{u} = e^{-ikz} A(\underbrace{e^{ikz}\tilde{u}}_u), \quad \tilde{u} = \tilde{u}(x, y, z),$$

where k corresponds to the wavenumber of the fundamental mode. Consequently, if original solution u involves the resolution of 10M wavelengths, the new variable \tilde{u} involves simulation of “only” 10k wavelengths, accessible with the parallel *hp3D* code [9, 12]. In context of the DPG method, the full envelope problem does not simply reduce to the use of the exponential ansatz; the new operator \tilde{A} is employed in the adjoint graph norm used in the actual computations.

Waveguide analysis. We have been able to analyze the stability of the (ideal) DPG full envelope waveguide model [16]. The result consists of three major steps. *Step 1:* Stability result for a (linear) acoustic or Maxwell waveguide problem with frequency ω and length L :

$$\|Au\| \geq \alpha\|u\|, \quad \alpha = \frac{C}{L}, \quad C > 0,$$

where $\|\cdot\|$ denotes the L^2 -norm. Note that the frequency is fixed and only the length of the waveguide (number of wavelengths) is varied. *Step 2:* Observation that operators A and \tilde{u} share the boundedness-below constant α ,

$$\|\tilde{A}\tilde{u}\| = \|e^{-ikz} A(e^{ikz}\tilde{u})\| = \|A(e^{ikz}\tilde{u})\| \geq \alpha\|e^{ikz}\tilde{u}\| = \alpha\|\tilde{u}\|.$$

Step 3: Dependence of the inf-sup constant for the ultraweak formulation upon α and a scaling constant β in the adjoint graph norm:

$$\sup_v \frac{(u, A^*v)}{\|v\|_V} = \sup_v \frac{(u, A^*v)}{\|A^*v\|} \frac{\|A^*v\|}{\sqrt{\|A^*v\|^2 + \beta^2\|v\|^2}} \geq \left(1 + \frac{\beta^2}{\alpha^2}\right)^{-1/2} \|u\|,$$

since operators A and A^* share the boundedness-below constant.

Acknowledgement. This work was partially supported by AFOSR grant #FA9550-19-1-0237 and NSF award #2103524.

REFERENCES

- [1] C. Carstensen, L. Demkowicz, J. Gopalakrishnan, *Breaking spaces and forms for the DPG method and applications including Maxwell equations*, *Comput. Math. Appl.* **72.3** (2016), 494–522.
- [2] L. Demkowicz, *Computing with hp Finite Elements. I. One and Two Dimensional Elliptic and Maxwell Problems*, Chapman & Hall/CRC Press, Taylor and Francis (2006).
- [3] L. Demkowicz, J. Kurtz, D. Pardo, M. Paszynski, W. Rachowicz, A. Zdunek, *Computing with hp Finite Elements. II. Frontiers: Three Dimensional Elliptic and Maxwell Problems with Applications*, Chapman & Hall/CRC (2007).
- [4] L. Demkowicz, J. Gopalakrishnan, *A class of discontinuous Petrov–Galerkin methods. II. Optimal test functions*, *Numer. Methods Partial Differ. Equ.* **27.1** (2011), 70–105.
- [5] L. Demkowicz, J. Gopalakrishnan, A. Niemi, *A class of discontinuous Petrov–Galerkin methods. Part III: adaptivity*, *Appl. Numer. Math.* **62.4** (2012), 396–427.
- [6] L. Demkowicz, J. Gopalakrishnan, *Discontinuous Petrov–Galerkin (DPG) method*, *Encyclopedia of Computational Mechanics Second Edition* (2017), 1–15.
- [7] F. Fuentes, B. Keith, L. Demkowicz, S. Nagaraj, *Orientation embedded high order shape functions for the exact sequence elements of all shapes*, *Comput. Math. Appl.* **70** (2015), 353–458.
- [8] J. Gopalakrishnan, W. Qiu, *An analysis of the practical DPG method*, *Math. Comput.* **83.286** (2014), 537–552.
- [9] S. Henneking, L. Demkowicz, *A numerical study of the pollution error and DPG adaptivity for long waveguide simulations*, *Comput. Math. Appl.* **95** (2021), 85–100.
- [10] S. Henneking, J. Grosek, L. Demkowicz, *Model and computational advancements to full vectorial Maxwell model for studying fiber amplifiers*, *Comput. Math. Appl.* **85** (2021), 30–41.
- [11] S. Henneking, *A scalable hp-adaptive finite element software with applications in fiber optics*, Ph.D. Thesis, The University of Texas at Austin (2021).
- [12] S. Henneking, J. Grosek, L. Demkowicz, *Parallel simulations of high-power optical fiber amplifiers*, *Lect. Notes Comput. Sci. Eng.* (accepted) (2022).
- [13] S. Henneking, L. Demkowicz, *hp3D User Manual*, arXiv preprint (2022), arxiv:2207.12211.
- [14] S. Henneking, L. Demkowicz, *Computing with hp Finite Elements. III. Parallel hp3D Code*, in preparation.
- [15] K. Kim, *Finite element modeling of electromagnetic radiation and induced heat transfer in the human body*, Ph.D. Thesis, The University of Texas at Austin (2013).
- [16] M. Melenk, L. Demkowicz, S. Henneking, *Convergence of full envelope DPG method for waveguide problems*, in preparation.
- [17] S. Petrides, L. Demkowicz, *An adaptive DPG method for high frequency time-harmonic wave propagation problems*, *Comput. Math. Appl.* **74.8** (2017), 1999–2017.
- [18] S. Petrides, *Adaptive multilevel solvers for the discontinuous Petrov–Galerkin method with an emphasis on high-frequency wave propagation problems*, Ph.D. Thesis, The University of Texas at Austin (2019).
- [19] S. Petrides, L. Demkowicz, *An adaptive multigrid solver for DPG methods with applications in linear acoustics and electromagnetics*, *Comput. Math. Appl.* **87** (2021), 12–26.

Discrete Vector Bundles with Connection and Curvature

ANIL N. HIRANI

(joint work with Daniel Berwick-Evans, Mark Schubel)

In the smooth theory of vector bundles with connection, spaces of vector bundle valued differential forms form a sequence with the operators between the pairs of spaces being d_{∇} , the exterior covariant derivative. This is in general a sequence, not a complex, since d_{∇}^2 is the curvature of the connection which need not be zero. The exterior covariant derivative is an extension of the connection on the vector bundle, similar to how d , the exterior derivative on scalar valued forms is an extension of the differential on smooth functions. Ordinary scalar valued forms act on vector bundle valued forms through linear maps and this action is the wedge product between scalar valued and vector bundle valued forms. The d_{∇} is compatible with d in that if w is a k -form on the base manifold and α is a vector bundle valued l -form then $d_{\nabla}(w \wedge \alpha) = dw \wedge \alpha + (-1)^{|w|} w \wedge d_{\nabla}\alpha$. That is, there is a product rule. The wedge and d_{∇} are natural with respect to pullbacks of bundles induced by smooth maps of the base manifolds.

What might a combinatorial version of this machinery look like? We have been developing something along these lines by generalizing discrete exterior calculus (DEC) to a framework for discrete vector bundle valued forms on an oriented manifold simplicial complex [1]. As in lattice gauge theory and in some other works on simplicial gauge theory [3], a vector space is associated with each vertex, and invertible parallel transport maps are associated with edges and constitute the discrete connection of the discrete bundle. By analogy with DEC, the discrete vector bundle valued k -forms are k -cochains. In the discrete vector bundle framework a k -cochain is a mapping from the k -simplices of the underlying simplicial complex X to vectors, one in each vector space associated with a vertex of each k -simplex. We call such a special vertex the origin vertex of that simplex.

These origin vertices are used as assembly points for the discrete operators and parallel transport maps are used to assemble quantities at the origin vertex. For example, the discrete d_{∇} is like the coboundary operator on cochains (which is used as a discrete exterior derivative in DEC), except that all vectors must be transported to the origin vertex, since vectors living in different vector spaces can't be added. We define $d_{\nabla}^2 := F$ to be the discrete curvature of the connection and this quantity measures the difference in transporting vectors along two paths on a triangle. Moreover, this d_{∇} is natural with respect to pullback via abstract simplicial maps of the base simplicial complexes. Thus abstract simplicial maps between simplicial complexes play the role of discrete smooth maps between manifolds as in DEC. The discrete d_{∇} has an extension that yields $d_{\nabla}F = 0$, a discrete Bianchi identity.

At this stage one has to make a choice about the origin vertices and consider alternatives to using vertices as assembly points. In the present framework, we have chosen to order the vertices of X and use the lowest numbered vertex in each simplex as the origin vertex. An alternative elegant choice is to associate

some point inside each simplex of each dimension as the assembly point. This latter approach is the one taken by [2]. In fact our approach and theirs can be related via a subdivision (this point was mentioned in passing during this talk). We were motivated to take a deeper look at the implications of vertex ordering and assembly points, prompted by discussions with Snorre Christiansen during the Newton Institute program in 2019.

Now a word about the discrete wedge product. In DEC, unlike in finite element exterior calculus (FEEC), cochains are not available as discrete forms defined everywhere in a simplex. In FEEC shape functions yield such discrete forms and thus one would imagine that taking a wedge product in FEEC is a simple matter. However, since polynomial spaces are not closed under products this requires more care. One approach for the lowest order FEEC (corresponding to, say, $P_1^- \Lambda^k$ spaces) is to use DEC for the wedge product and then interpolate using shape functions. Indeed, for some purposes DEC can be viewed as a computational framework working exclusively with degrees of freedom corresponding of the lowest order FEEC. Thus it seems worthwhile for DEC and its extensions to confront the question of products in order to discretize product terms such as that arising in the convection term in Navier-Stokes equations. In DEC a cup-like product on cochains is analogous to the tensor product and it is anti-symmetrized to define a discrete wedge product. This discrete wedge product is also natural with respect to pullbacks via abstract simplicial maps.

In extending these ideas to vector bundle valued cochains we discovered the following curious fact. We found that if assembly points are chosen to be inside each simplex then a product rule for cup-like product is obstructed by curvature. If the assembly points are chosen as the lowest numbered vertices in each simplex then a cup-like product does satisfy a product rule. However some terms in the anti-symmetrization will have a curvature obstruction in the product rule. As a result we are currently studying the implications of using a cup-like product without anti-symmetrization as a discrete wedge product for discrete vector bundles with connection.

REFERENCES

- [1] D. Berwick-Evans, A. N. Hirani, M. Schubel. *Discrete vector bundles with connection and the Bianchi identity*, arXiv:2104.10277 [math.DG] (2021).
- [2] S. H. Christiansen, K. Hu. *Finite element systems for vector bundles: elasticity and curvature*, Foundations of Computational Mathematics, (2022), DOI:10.1007/s10208-022-09555-x.
- [3] S. H. Christiansen, T. G. Halvorsen. *A simplicial gauge theory*, J. Math. Phys. **53** (2012), DOI:10.1063/1.3692167.

Geometric finite elements for nonlinear Cosserat shell problems

OLIVER SANDER

(joint work with Hanne Hardering, Lisa Julia Nebel, and Patrizio Neff)

We discuss structure-preserving discretizations for problems involving maps $v : \omega \rightarrow M$ between manifolds ω and M . The prime example of such a problem is the computation of harmonic maps from ω to M , that is, maps that make the Dirichlet energy

$$J(v) = \int_{\omega} \|\nabla v\|^2 dx$$

stationary.

Discretizing such problems is challenging because M typically does not have a vector space structure. Therefore the typical approximations by finite elements (i.e., piecewise polynomials) is not possible. To preserve the nonlinear structure of sets of maps into M , we present two types of generalized finite element functions [3]. These functions v_h , collectively termed *geometric finite elements*, are geometrically conforming in the sense that $v_h(x) \in M$ for each $x \in \omega$. At the same time, they degenerate to classical piecewise polynomials in the special case $M = \mathbb{R}$. What is more, geometric finite elements are Sobolev functions, i.e., elements of $H^1(\omega; M)$. This simplifies the error analysis of corresponding numerical methods for solving partial differential equations tremendously. The finite elements are constructed either by projecting polynomials in a surrounding space pointwise onto M (*projection-based finite elements*), or intrinsically by using the Riemannian center of mass (*geodesic finite elements*). These constructions preserve all invariance properties expected by applications in physics and mechanics.

For the harmonic maps problem we show a priori bounds of the discretization error in the H^1 and L^2 norms. The bounds are optimal in the sense that the discretization errors are bounded by the same powers of the mesh resolution as in linear problems in vector spaces. We also verified this numerically. The proofs generalize established constructs from the vector space theory such as the Céa lemma and the Aubin–Nitsche trick to the non-Euclidean setting. Approximation properties of the nonlinear finite element spaces are shown under four abstract conditions, which are fulfilled by the particular constructions mentioned above.

We apply the novel discretization technique to an advanced elastic Cosserat shell model, generalizing a model originally proposed in [1]. Such a shell model describes the mechanical behavior of thin, essentially two-dimensional objects under load. In our generalization, the midsurface of the shell is an abstract smooth twodimensional manifold ω . A configuration is given as an immersion $\mathbf{m} : \omega \rightarrow \mathbb{R}^3$ together with a field of orientations $\mathbf{Q}_e : \omega \rightarrow \text{SO}(3)$, which describes local shearing and drilling of the shell. The material behavior is described by a hyperelastic energy density involving terms up to fifth order in the shell thickness. For shells that are homeomorphic to a subset of \mathbb{R}^2 , Ghiba et al. [2] proved existence of global minimizers of the shell energy in $H^1(\omega; \mathbb{R}^3 \times \text{SO}(3))$. We generalize the result to general midsurfaces ω .

We compute numerical solutions of this model. Geodesic finite elements are used to approximate the microrotation field \mathbf{Q}_e , whereas the midsurface configuration \mathbf{m} is approximated with standard Lagrange finite elements. We prove that this discrete problem has at least one solution. Numerically we show that the model does not show shear locking, unless the approximation orders of the fields and of the geometry are too low. We also show that the discrete model can reproduce challenging wrinkling and buckling scenarios.

REFERENCES

- [1] I.–D. Ghiba, M. Birsan, P. Lewintan, and P. Neff, *The isotropic Cosserat shell model including terms up to $O(h^5)$. Part I: Derivation in matrix notation*, Journal of Elasticity **142** (2020), 201–262.
- [2] I.–D. Ghiba, M. Birsan, P. Lewintan, and P. Neff, *The isotropic Cosserat shell model including terms up to $O(h^5)$. Part II: Existence of Minimizers*, Journal of Elasticity **142** (2020), 263–290.
- [3] H. Hardering and O. Sander, *Geometric Finite Elements*, in *Handbook of Variational Methods for Nonlinear Geometric Data*, Springer, edited by P. Grohs, M. Holler, and A. Weinmann, (2020), pages 3–49.

Numerical Simulation of Wave Equations

SANNA MÖNKÖLÄ

(joint work with Lauri Kettunen, Tuomo Rossi, Jukka Rabinä, Tytti Saksa, and Jonni Lohi)

We present a general model for linear wave equations covering hyperbolic problems in both classical and quantum mechanical application areas. The model is based on differential geometry in $(d + 1)$ -dimensional spacetime. We discretize the problem in spacetime with the discrete exterior calculus and run numerical simulations using a software library developed at the University of Jyväskylä.

1. MODEL

We present a general model for linear wave equations in four dimensions based on a Clifford algebra in Minkowski spacetime $\mathbb{R}^{1,d}$. That is, we have an Euclidean space $(x_1, x_2, \dots, x_d)^T$, imaginary time $x_0 = ict$, and orthonormal basis vectors γ_i , $i = 0, \dots, d$, such that $\gamma_0\gamma_0 = -1$ and $\gamma_i\gamma_i = 1$ for $i = 1, \dots, d$. The unit pseudoscalar is $i = \gamma_0\gamma_1 \cdots \gamma_d$. The geometric product of two vectors, a and b , can be presented by $ab = a \cdot b + a \wedge b$, where $a \cdot b$ is the dot product and $a \wedge b = ia \times b$ is the exterior product (wedge product). The geometric product of the basis vectors is associative and distributive, and $\gamma_i\gamma_j = -\gamma_j\gamma_i$ for $i \neq j$.

The basis for $(1+d)$ -dimensional geometric algebra is set by 2^{d+1} blades.

Basis k -blades (of grade k) are wedge products of k basis vectors that span a k -dimensional subspace. The wedge product of two vectors results to a two-dimensional subspace called bivector (2-vector), the wedge product of three vectors results to a three-dimensional subspace called trivector (3-vector), and so forth. In a four-dimensional space, the basis is set by $2^4 = 16$ blades, and a general element

$F = f_1 + f_2\gamma_0 + f_3\gamma_1 + f_4\gamma_2 + f_5\gamma_3 + f_6(\gamma_0 \wedge \gamma_1) + f_7(\gamma_0 \wedge \gamma_2) + f_8(\gamma_0 \wedge \gamma_3) + f_{11}(\gamma_2 \wedge \gamma_3) + f_{10}(\gamma_3 \wedge \gamma_1) + f_9(\gamma_1 \wedge \gamma_2) + f_{14}(\gamma_0 \wedge \gamma_2 \wedge \gamma_3) + f_{13}(\gamma_0 \wedge \gamma_3 \wedge \gamma_1) + f_{12}(\gamma_0 \wedge \gamma_1 \wedge \gamma_2) + f_{15}(\gamma_1 \wedge \gamma_2 \wedge \gamma_3) + f_{16}(\gamma_0 \wedge \gamma_1 \wedge \gamma_2 \wedge \gamma_3)$ is presented as a sum of blades weighted by coefficients $f_i, i = 1, \dots, 16$. Respectively, we present a general source J . F is operated by the spacetime gradient $\nabla = -\gamma_0\partial_0 + \gamma_1\partial_1 + \gamma_2\partial_2 + \gamma_3\partial_3$, and the resulting multivector is equal to 0 in free space or $J \neq 0$ with external forces. The resulting system resembles Rainer Picard's "Mother PDE" [5].

Based on the dual correspondence between k -vectors and k -differential forms [1], we turn to a differential form representation, where the differentials dx^0, dx^1, dx^2 and dx^3 are basis 1-forms and basis k -forms are constructed as wedge (exterior) products of k basis 1-forms, such that, $dx^i \wedge dx^i = 0$ and $dx^i \wedge dx^j = -dx^j \wedge dx^i$. With differential (multi)forms \tilde{F} and \tilde{J} we can present linear wave models as $\partial\tilde{F} = \tilde{J}$, or $\partial \star \tilde{F} = \star \tilde{J}$, where $\partial = (\mathbf{d} + \boldsymbol{\delta})$ is the differential operator that is the sum of the exterior derivative \mathbf{d} and its coderivative (interior derivative) $\boldsymbol{\delta} = (-1)^k \star^{-1} \mathbf{d} \star$ and \star is the Hodge star operator. See [4] for the action principle based derivation of the general model and topical physics field models as its instances.

2. DISCRETIZATION

We perform the spacetime discretization by the discrete exterior calculus (DEC) method. In principle, the procedure is similar than applied to space discretization (see, e.g. [2, 7, 8]). First, we provide the computational domain with two meshes, a primal mesh and a dual mesh. The dual mesh is orthogonal, under the Minkowski inner product, to the primal mesh. Each mesh is a cell complex with such a hierarchy that a 0-cell is a vertex, a 1-cell is an edge between two 0-cells, a 2-cell is a face surrounded by edges, a 3-cell is a volume element surrounded by faces, and a 4-cell is a 4D volume element. Each primal k -cell is associated with a corresponding dual $(n - k)$ -cell. The variables can be associated with nodes (0-forms), edges (1-forms), faces (2-forms), volumes (3-forms), or 4-volumes (4-forms).

A discrete k -form corresponding to a differential form α_k is

$$(1) \quad u_k = \int_{\mathcal{C}_k} \alpha_k = \begin{pmatrix} \int_{\mathcal{C}_{k_1}} \alpha_k \\ \vdots \\ \int_{\mathcal{C}_{k_{n_p}}} \alpha_k \end{pmatrix},$$

where \mathcal{C}_{ki} is the i th k -cell and n_p is the number of k -cells in the mesh. At the discrete level, the exterior derivative is presented as an incidence matrix d_k that operates discrete differential k -forms u_k and represents the neighboring relations and relative orientations. Since the Stokes theorem holds exactly, $d_k u_k = d_k \int_{\mathcal{C}_k} \alpha_k = \int_{\mathcal{C}_{k+1}} d\alpha_k$, the discrete differential operator is exact. The discrete counterpart to the Hodge operator is matrix \star_k mapping between the primal and dual mesh. It is diagonal by construction if the dual elements are orthogonal to the primal elements.

The discretized general model for linear wave equations in four dimensions without external forces is

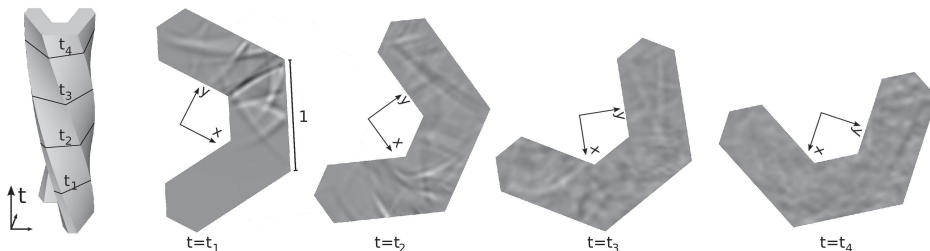
$$(2) \quad \begin{pmatrix} & \delta_{0s} & \frac{1}{\Delta t^2} d_{0t} & & & \\ d_{0s} & & & & & \\ d_{0t} & & & & & \\ & d_{1s} & & & & \\ & d_{1t} & -d_{0s} & & & \\ & & & & & \\ & & & d_{2s} & \frac{1}{\Delta t^2} d_{2t} & \\ & & & & -\delta_{1s} & \\ & & & & & \\ & & & d_{2s} & & \frac{1}{\Delta t^2} d_{3t} \\ & & & d_{2t} & -d_{1s} & -\delta_{2s} \\ & & & & & \\ & & & & & \\ & & & d_{3t} & -d_{2s} & \end{pmatrix} \begin{pmatrix} u_{0s} \\ u_{1s} \\ u_{1t} \\ u_{2s} \\ u_{2t} \\ u_{3s} \\ u_{3t} \\ u_{4t} \end{pmatrix} = 0,$$

where discrete k -forms u_k and incidence matrices d_k and the corresponding co-operators δ_k are constructed by spatial (subscript s) and temporal (subscript t) components. As a consequence of the model (2), we get a leap-frog style time-stepping.

3. NUMERICAL EXAMPLES

As an example we consider a spacetime mesh twisted around the time axis making the cross-section of a boomerang shaped cavity to rotate. The primal mesh is constructed by simplices and it has 29952 nodes, 194068 edges, 320834 faces, and 156717 volumes. The wave source is set in the beginning of the simulation by discrete 2-form values on the mesh faces whose center of the mass is closer than the distance of $\frac{\pi}{50}$ to the point that is at horizontal distance of 12 edges from the tip of the trailing boomerang arm.

The boundaries of the cavity are assumed to be rigid. The simulation was carried out with the wave speed 1 until time $t = 7.2$ reached. The snapshots of total wave pattern, as the wave is scattered by the moving cavity boundaries, are presented in the figure below at $t = t_i = \frac{9i}{5}$, $i = 1, 2, 3, 4$. The CPU time required for the simulation, including mesh generation, assembling discrete structures, spacetime evolution, and visualization, was 145 s on an Intel Core i5-5300U processor at 2.30 GHz. Moving or deforming domains can be obtained by the construction in (1+1)- and (3+1)-dimensional cases [6], as well. The future work includes higher-order DEC-based discretizations [3] in spacetime.



REFERENCES

- [1] F. Brackx, R. Delanghe, F. Sommen, *Differential forms and/or multi-vector functions*, *Cubo*, A Mathematical Journal, 7(2) (2005), 139–169.
- [2] M. Desbrun, A. N. Hirani, J. E. Marsden, *Discrete exterior calculus for variational problems in computer vision and graphics*, In 42nd IEEE International Conference on Decision and Control, vol. 5, (2003), 4902–4907.
- [3] L. Kettunen, J. Lohi, J. Rabinä, S. Mönkölä, T. Rossi, *Generalized finite difference schemes with higher order Whitney forms*, *ESAIM: Mathematical Modelling and Numerical Analysis*, 55(4) (2021).
- [4] L. Kettunen, S. Mönkölä, J. Parkkonen, T. Rossi, *General conservation law for a class of physics field theories*, arXiv preprint arXiv:1908.10634.
- [5] R. Picard, *Mother operators and their descendants*, *Journal of Mathematical Analysis and Applications*, 403.1 (2013), 54–62.
- [6] T. Rossi, J. Rabinä, S. Mönkölä, S. Kiiskinen, J. Lohi L. Kettunen, *Systematisation of systems solving physics boundary value problems*, In *Proceeding of the European Numerical Mathematics and Advanced Applications Conference*, Springer, (2021) 35–51.
- [7] J. Rabinä, S. Mönkölä, T. Rossi, *Efficient time integration of Maxwell’s equations with generalized finite differences*, *SIAM Journal on Scientific Computing*, 37(6) (2015) B834–B854.
- [8] J. Rabinä, L. Kettunen, S. Mönkölä, T. Rossi, *Generalized wave propagation problems and discrete exterior calculus*, *ESAIM: Mathematical Modelling and Numerical Analysis*, 52(3) (2018) 1195–1218.

Towards “all” boundary value problems – exploitation of the structural properties

LAURI KETTUNEN, TUOMO ROSSI

Second order boundary value problems and their numerical solutions provide one with a powerful design tool. In developing tools for design, it would be very inefficient to create software for each specific need, but instead, one is after a concise system that served many purposes at once. This raises a mathematical question: What is the common structure behind second order boundary value problems, and how should this structure be represented in finite dimensional spaces (in which the problems are solved)?

This question boils down to analogies and quoting John Baez, “every good analogy is yearning to become a functor”. Functors are mappings between categories such that the compositions and identity morphisms are preserved. Boundary value problems themselves contain a i) structural layer of differentiability – for this only a sufficiently smooth manifold is needed – and ii) the metric dependent layer. The differentiable structure is given by pairs of differential equations, and the metric layer is established with the constitutive laws. The modern view on differential equations is, they are derived from the action principle.

“All” boundary value problems point to a class rather than a finite set. Exploitation of the structural properties means, one works out a type of boundary value problem – for example, say Maxwell’s equations – as a category. Then, if one finds a functor to other type of problems – such as to those of elasticity – by definition, the functor preserves the compositions of the underlying morphism,

here, the compositions of the functions. This then reveals and answers the question, which functions are the ones that should be translated to pieces of software to build multipurpose software. Notice, all software programs are functions as indicated by functional programming languages.

The presentation explains an approach to find some basic structural blocks behind the commonly employed field theories of physics. As a pragmatic example, we explain how one may construct a generalized pair of partial differential equations. This yields foundations to software systems that are not restricted to particular or a priori given problems.

REFERENCES

- [1] L. Kettunen, J. Lohi, J. Rabinä, S. Mönkölä, T. Rossi, *Generalized finite difference schemes with higher order Whitney formse*, ESAIM Mathematical Modelling and Numerical Analysis **55** (2021).
- [2] L. Kettunen, S. Mönkölä, J. Parkkonen, T. Rossi, *General conservation law for a class of physics field theories*, arXiv:1908.10634.

Participants

Prof. Dr. Ana Alonso Rodriguez

Dipartimento di Matematica
Università degli Studi di Trento
Via Sommarive, 14
38123 Povo (TN)
ITALY

Prof. Dr. Paola F. Antonietti

MOX-Laboratory for Modeling and
Scientific Computing
Dipartimento di Matematica
Politecnico di Milano
Piazza Leonardo da Vinci 32
20133 Milano
ITALY

Prof. Dr. Douglas N. Arnold

School of Mathematics
University of Minnesota
512 Vincent Hall 206 Church St.SE
Minneapolis MN 55455
UNITED STATES

Prof. Dr. Lourenco Beirao da Vega

Dip. di Matematica e Applicazioni
Universita di Milano-Bicocca
Edificio U5
via Roberto Cozzi 53
20125 Milano
ITALY

Dr. Yakov Berchenko-Kogan

Department of Mathematics
Pennsylvania State University
University Park, PA 16802
UNITED STATES

Prof. Dr. Fleurianne Bertrand

Department of Mathematics
and Computer Science
University of Twente
P.O. Box 217
7500 AE Enschede
NETHERLANDS

Prof. Dr. Daniele Boffi

Computer, Electrical and Mathematical
Sciences and Engineering Division
King Abdullah University of Science and
Technology (KAUST)
23955-6900 Thuwal
SAUDI ARABIA

Dr. Francesca Bonizzoni

Institut für Mathematik
Universität Augsburg
86135 Augsburg
GERMANY

Dr. Wietse Boon

Department of Mathematics
KTH
10044 Stockholm
SWEDEN

Prof. Dr. Alain Bossavit

Laboratoire de Genie Electrique
de Paris (LGEP), Supelec
Universités Paris VI et Paris XI
11, Rue Joliot-Curie
91192 Gif-sur-Yvette -CEDEX
FRANCE

Prof. Dr. Dietrich Braess

Fakultät für Mathematik
Ruhr-Universität Bochum
44780 Bochum
GERMANY

Prof. Dr. Annalisa Buffa

EPFL SB MATH MNS
MA C2 573
Station 8
1015 Lausanne
SWITZERLAND

Prof. Dr. Andreas Cap

Institut für Mathematik
Universität Wien
Oskar-Morgenstern-Platz 1
1090 Wien
AUSTRIA

Prof. Dr. Long Chen

Department of Mathematics
University of California, Irvine
11 Mistral Lane
Irvine, CA 92617
UNITED STATES

**Prof. Dr. Snorre Harald
Christiansen**

Department of Mathematics
University of Oslo
P.O.Box 1053 - Blindern
0316 Oslo
NORWAY

Prof. Dr. Philippe G. Ciarlet

Department of Mathematics
City University of Hong Kong
Academic Building
83 Tat Chee Avenue
Kowloon Tong
HONG KONG

Prof. Dr. Martin Costabel

Département de Mathématiques
Université de Rennes I
Campus de Beaulieu
35042 Rennes Cedex
FRANCE

Prof. Dr. Franco Dassi

Dipartimento di Matematica e
Applicazioni
Università degli Studi di Milano-Bicocca
Via Cozzi 55
20125 Milano
ITALY

Prof. Dr. Monique Dauge

IRMAR
Université de Rennes I
Campus de Beaulieu
35042 Rennes Cedex
FRANCE

Prof. Dr. Leszek F. Demkowicz

Oden Institute for Computational
Engineering and Sciences (OICES)
University of Texas at Austin
1 University Station C
Austin, TX 78712-1085
UNITED STATES

Prof. Dr. Alan Demlow

Department of Mathematics
Texas A & M University
Mail Stop 3368
College Station, TX 77843-3368
UNITED STATES

Prof. Dr. Daniele Di Pietro

IMAG, University of Montpellier
Place Eugene Bataillon
34095 Montpellier Cedex 5
FRANCE

Prof. Dr. Michael Dumbser

DICAM
Università degli Studi di Trento
Via Mesiano, 77
38123 Trento
ITALY

Dr. Andrea Dziubek

Department of Mathematics
State University of New York
Polytechnic Institute at Utica
100 Seymour Rd
Albany, NY 13502
UNITED STATES

Prof. Dr. Michael Eastwood

School of Mathematical Sciences,
University of Adelaide
Adelaide SA 5005
AUSTRALIA

Prof. Dr. Herbert Egger

Institut für Numerische Mathematik
Johannes Kepler Universität Linz
Altenberger Str. 69
4040 Linz
AUSTRIA

Dr. Bernhard Endtmayer

Institut für Angewandte Mathematik
Leibniz Universität Hannover
Welfengarten 1
30167 Hannover
GERMANY

Prof. Dr. Richard S. Falk

Department of Mathematics
Rutgers University
Hill Center, Busch Campus
110 Frelinghuysen Road
Piscataway, NJ 08854-8019
UNITED STATES

Bernt Jonas Flode

Department of Mathematics
University of Oslo
P. O. Box 1053 - Blindern
0316 Oslo
NORWAY

Evan Gawlik

Department of Mathematics
University of Hawaii at Manoa
2565 McCarthy Mall, Keller Hall 401A
Honolulu, Hawaii 96822
UNITED STATES

Prof. Dr. Jay Gopalakrishnan

Portland State University
P.O. Box 751
OR Portland OR 97207-0751
UNITED STATES

Prof. Dr. Johnny Guzman

Division of Applied Mathematics
Brown University
Box F
182 George Str.
Providence, RI 02912
UNITED STATES

Dr. Julia Hauser

Abteilung Mathematik
Technische Universität Dresden
01062 Dresden
GERMANY

Prof. Dr. Ralf Hiptmair

Seminar für Angewandte Mathematik
ETH - Zentrum
Rämistrasse 101
8092 Zürich
SWITZERLAND

Prof. Dr. Anil N. Hirani

Department of Mathematics
University of Illinois at
Urbana-Champaign
1409 W. Green Street
Urbana, IL 61801
UNITED STATES

Daniel Forland Holmen

Department of Mathematics
University of Bergen
Allégaten 41
5007 Bergen
NORWAY

Prof. Dr. Michael Holst

Department of Mathematics
University of California, San Diego
9500 Gilman Drive
La Jolla, CA 92093-0112
UNITED STATES

Prof. Dr. Jun Hu

School of Mathematical Sciences
Peking University
No. 5 Yiheyuan Road
Beijing 100 871
CHINA

Dr. Kaibo Hu

Mathematical Institute
Oxford University
Andrew Wiles Building
Oxford OX2 6GG
UNITED KINGDOM

Prof. Dr. Xuehai Huang

Red Tile Building
Shanghai University of Finance and
Economics
777 Guoding Road
200433 Shanghai Shi
CHINA

Prof. Dr. Lauri Kettunen

Faculty of Information Technology
University of Jyväskylä
Agora, Mattilanniemi 2
P.O. Box P.O.Box 35
40014 Jyväskylä
FINLAND

Prof. Dr. Stefan Kurz

c/o Prof. Lauri Kettunen
Department of Mathematics
University of Jyväskylä
Seminaarinkatu 15
40100 Jyväskylä
FINLAND

Dr. Martin Licht

EPFL SB MATH-GE
Martin Licht
MA A1 364, Bât. MA
Station 8
1015 Lausanne
Switzerland
1015 Lausanne
SWITZERLAND

Prof. Dr. Peter Monk

Department of Mathematical Sciences
University of Delaware
Newark DE 19716-2553
UNITED STATES

Dr. Sanna Mönkölä

Faculty of Information Technology
University of Jyväskylä
Mattilanniemi 2
P.O. Box P.O. Box 35
40014 Jyväskylä
FINLAND

Prof. Dr. Michael J. Neilan

Department of Mathematics
University of Pittsburgh
139 University Place
Pittsburgh PA 15260
UNITED STATES

Dr. Michael Neunteufel

Institut für Analysis und
Scientific Computing
Technische Universität Wien
Wiedner Hauptstraße 8 - 10
1040 Wien
AUSTRIA

Dr. Minah Oh

Dept. of Mathematics and Statistics
James Madison University
305 Roop Hall, MSC 1911, 60 Bluestone
Dr
22807 Harrisonburg VA 22807
UNITED STATES

Prof. Dr. Dirk Pauly

Institut für Analysis
Fakultät Mathematik
Technische Universität Dresden
Zellescher Weg 12-14
01069 Dresden
GERMANY

Prof. Dr. Astrid Pechstein

Institut für Technische Mechanik
Johannes Kepler Universität
Altenberger Str. 69
4040 Linz
AUSTRIA

Prof. Dr. Rainer Picard

Institut für Analysis
Fachrichtung Mathematik
Technische Universität Dresden
01062 Dresden
GERMANY

Prof. Dr. Francesca Rapetti

Laboratoire J.-A. Dieudonné
UMR CNRS 6621
Université de Nice Sophia-Antipolis
Parc Valrose
06108 Nice Cedex 2
FRANCE

Prof. Dr. Tuomo Rossi

Faculty of Information Technology
University of Jyväskylä
Mattiilanniemi 2
40100 Jyväskylä
FINLAND

Prof. Dr. Alessandro Russo

Dipartimento di Matematica
Università Milano-Bicocca
Via Cozzi 55
20126 Milano
ITALY

Dr. Espen Sande

Section de Mathématiques
Station 8
École Polytechnique Fédérale de
Lausanne
1015 Lausanne
SWITZERLAND

Prof. Dr. Oliver Sander

Institut für Numerische Mathematik
Technische Universität Dresden
Zellescher Weg 12-14
01069 Dresden
GERMANY

Prof. Dr. Joachim Schöberl

Institut für Analysis und
Scientific Computing
Technische Universität Wien
Wiedner Hauptstraße 8 - 10
1040 Wien
AUSTRIA

Michael Schomburg

Fakultät für Mathematik
Universität Duisburg-Essen
45117 Essen
GERMANY

Erick Schulz

Département Mathematik
ETH-Zentrum
Rämistr. 101
8092 Zürich
SWITZERLAND

Prof. Dr. Ari Stern

Department of Mathematics and
Statistics
Washington University in St. Louis
Campus Box 1146
One Brookings Drive
St. Louis, MO 63130-4899
UNITED STATES

Dr. Sascha Trostorff

Mathematisches Seminar
Christian-Albrechts-Universität Kiel
Ludewig-Meyn-Str. 4
24118 Kiel
GERMANY

Prof. Dr. Alberto Valli

Dipartimento di Matematica
Università degli Studi di Trento
Via Sommarive, 14
38123 Povo (TN)
ITALY

Prof. Dr. Nicolas van Goethem

Department of Mathematics
University of Lisboa
R. Ernesto Vasconcelos B1
C1-Piso 3
1700 Lisboa Codex
PORTUGAL

Dr. Wei Wang

School of Mathematics
University of Minnesota
Vincent Hall 206 Church St. SE
Minneapolis MN 55455
UNITED STATES

Prof. Dr. Lucy Weggler

Hochschule für Technik und Wirtschaft
Wilhelminenhofstraße 75A
12459 Berlin
GERMANY

Prof. Dr. Ragnar Winther

Department of Mathematics,
University of Oslo
Blindern
P.O. Box 1053
0316 Oslo
NORWAY

Prof. Dr. Jinchao Xu Jinchao Xu

Department of Mathematics
Pennsylvania State University
University Park PA 16802
UNITED STATES

Dr. Michele Zaccaron

Dipartimento di Matematica
Università di Padova
Via Trieste, 63
35121 Padova
ITALY

Dr. Enrico Zampa

Dipartimento di Matematica
Universita di Trento
Via Sommarive 14
38050 Povo (Trento)
ITALY

Prof. Dr. Walter Zulehner

Radon Institute for Computational and
Applied Mathematics
of the Austrian Academy of Sciences
Altenbergerstr. 69
4040 Linz
AUSTRIA

